US 20100201205A1

(19) **United States**

(12) **Patent Application Publication**

(10) **Pub. No.: US 2010/0201205 A1**

(43) **Pub. Date: Aug. 12, 2010**

Karalis et al.

(54) **BIOLOGICAL EFFECTS OF MAGNETIC POWER TRANSFER**

(76) Inventors: **Aristeidis Karalis**, Boston, MA (US); **Andre B. Kurs**, Chestnut Hill, MA (US); **Robert Moffatt**, Reston, VA (US); **John D. Joannopoulos**, Belmont, MA (US); **Peter H. Fisher**, Cambridge, MA (US); **Marin Soljacic**, Belmont, MA (US)

Correspondence Address:
GTC Law Group LLP & Affiliates
P.O. Box 113237
Pittsburgh, PA 15241 (US)

(21) Appl. No.: **12/766,232**

(22) Filed: **Apr. 23, 2010**

Related U.S. Application Data

(63) Continuation of application No. 12/688,339, filed on Jan. 15, 2010, which is a continuation of application No. 12/055,963, filed on Mar. 26, 2008, which is a continuation-in-part of application No. 11/481,077, filed on Jul. 5, 2006, now Pat. No. 7,741,734, said application No. 12/055,963 is a continuation-in-part of application No. PCT/US2007/070892, filed on Jun. 11, 2007.

(60) Provisional application No. 60/908,383, filed on Mar. 27, 2007, provisional application No. 60/908,666, filed on Mar. 28, 2007, provisional application No. 60/698,442, filed on Jul. 12, 2005, provisional application No. 60/908,383, filed on Mar. 27, 2007, provisional application No. 60/908,666, filed on Mar. 28, 2007.

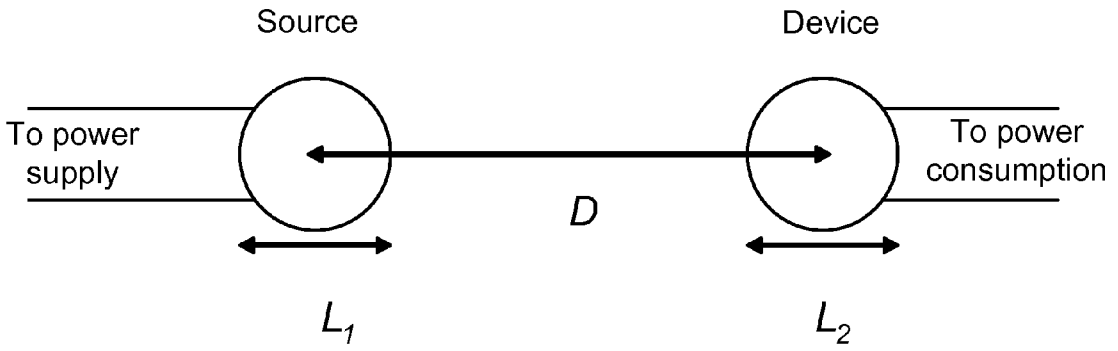
Publication Classification

(51) **Int. Cl.**
H02J 17/00 (2006.01)

(52) **U.S. Cl.** **307/104**

(57) **ABSTRACT**

Described herein are embodiments of forming a wireless power transfer system which uses at least two high-Q magnetically resonant elements, and which have values which are set to acceptable levels of electric and magnetic field strength and radiated power.



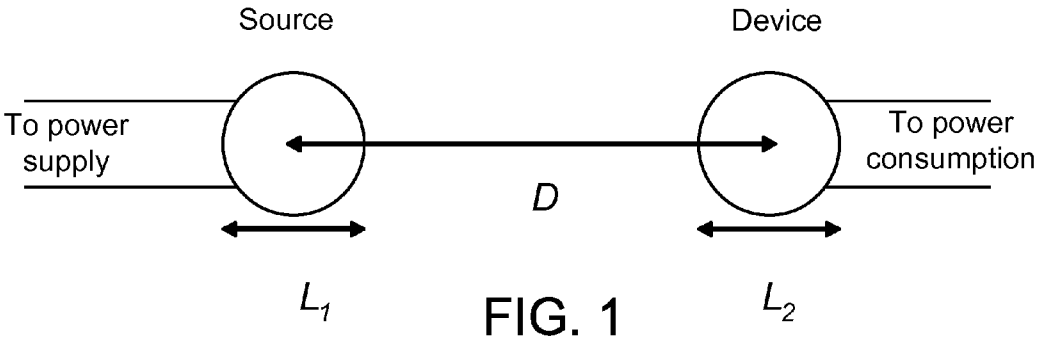


FIG. 1

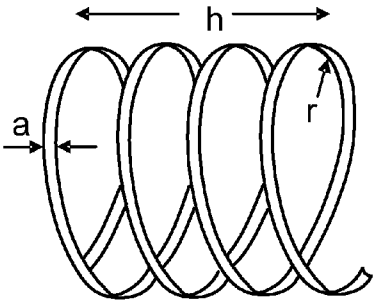


FIG. 2

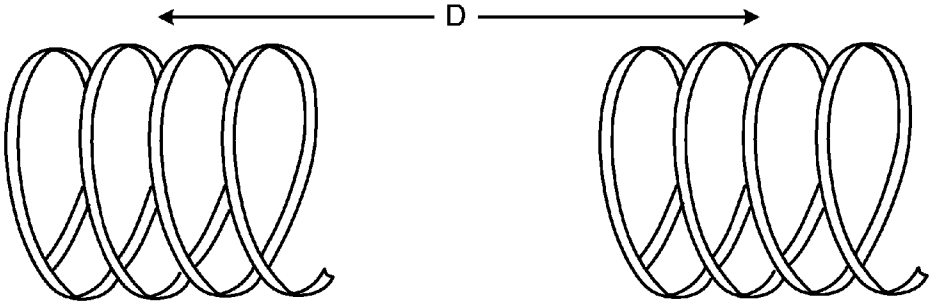


FIG. 3

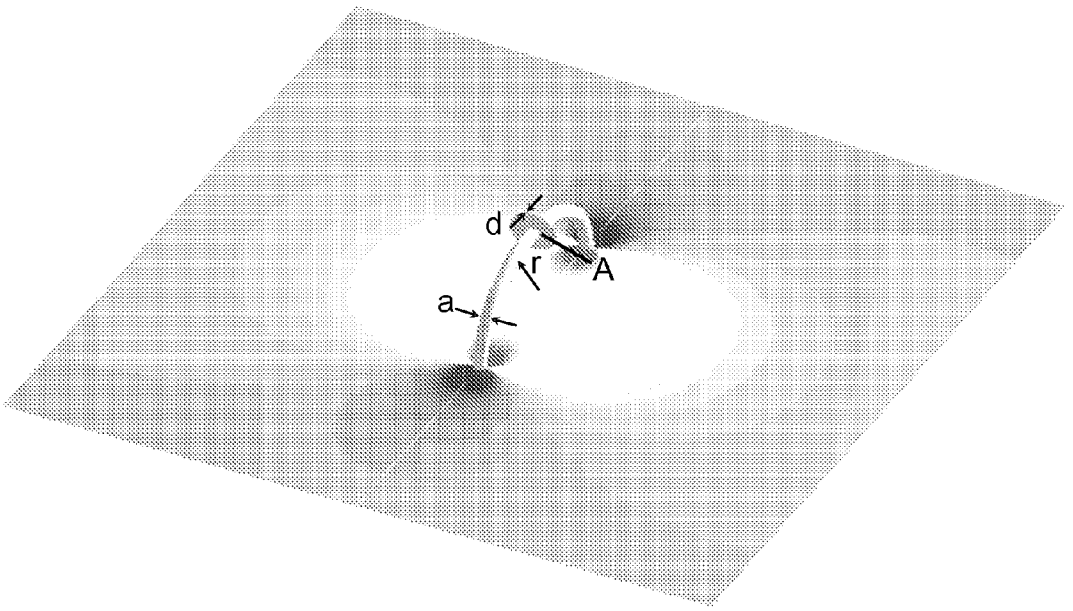


FIG. 4

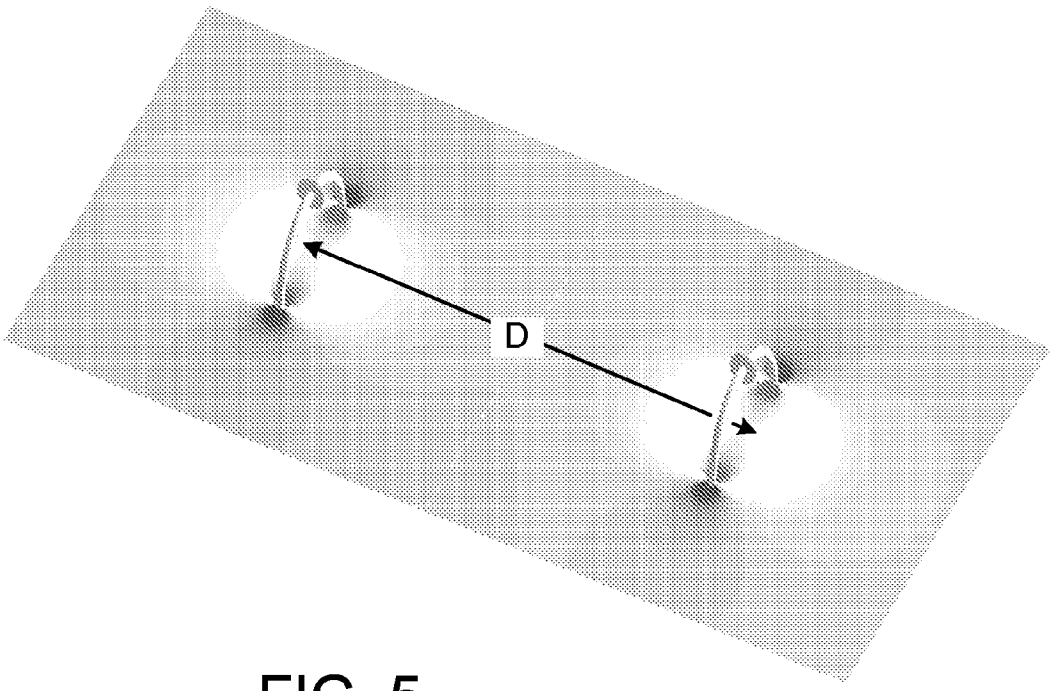


FIG. 5

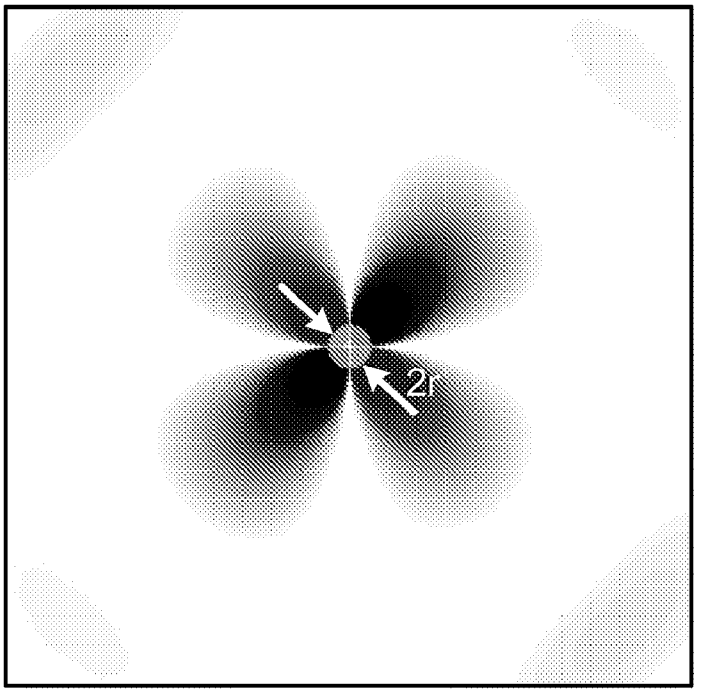


FIG. 6

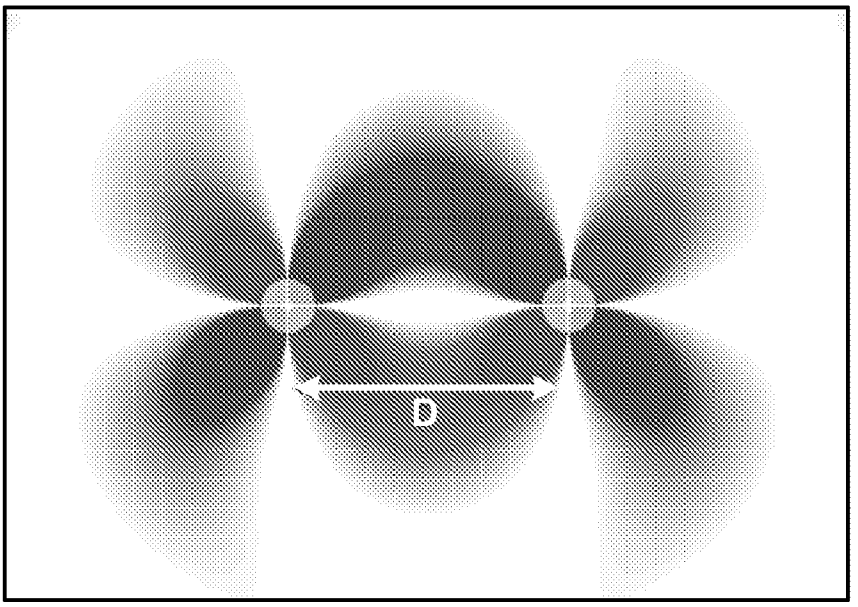


FIG. 7

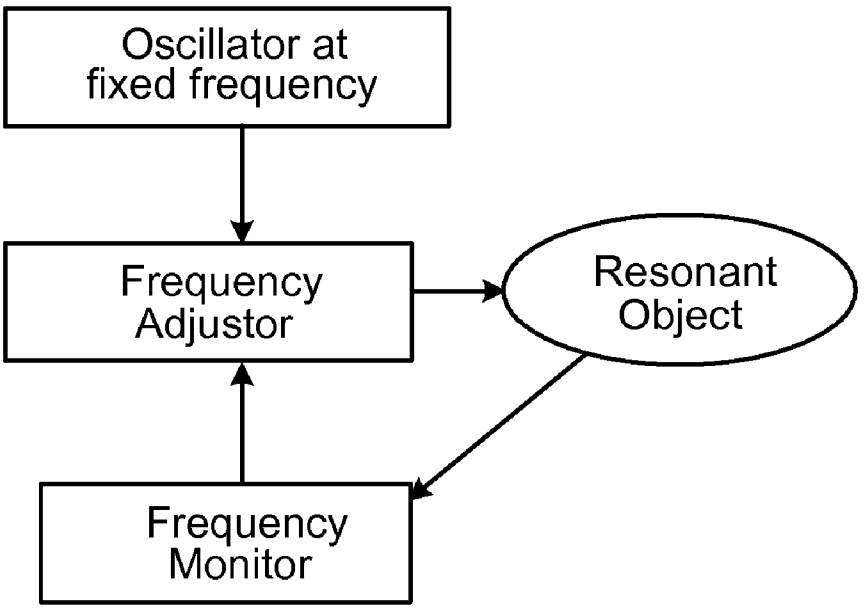

Oscillator at fixed frequency
Frequency Adjustor
Resonant Object
Frequency Monitor

FIG. 8A

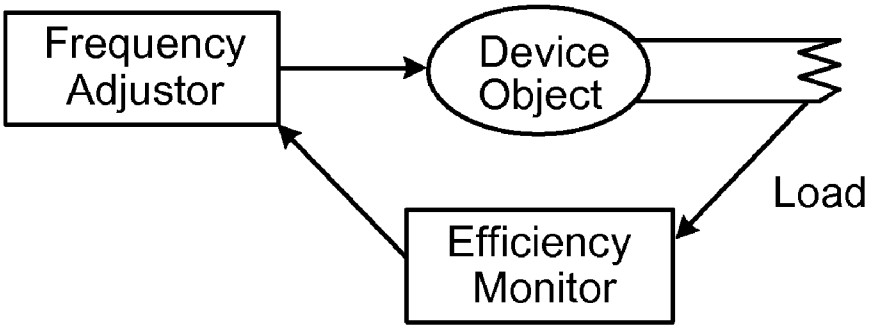
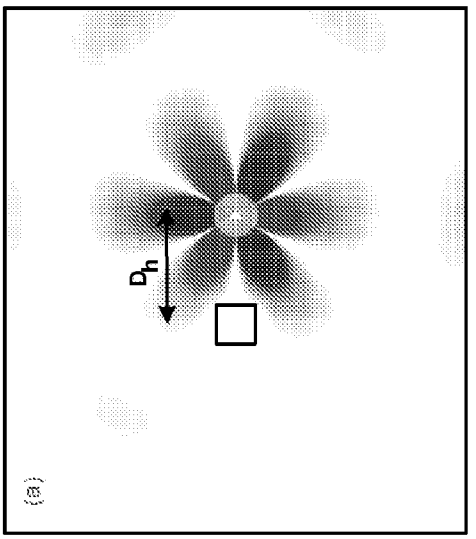
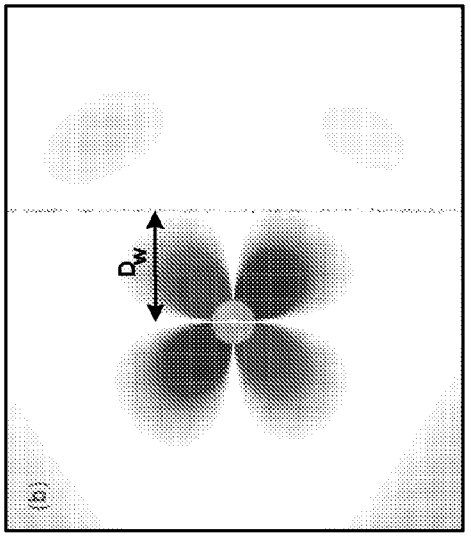

Frequency Adjustor
Device Object
Load
Efficiency Monitor

FIG. 8B



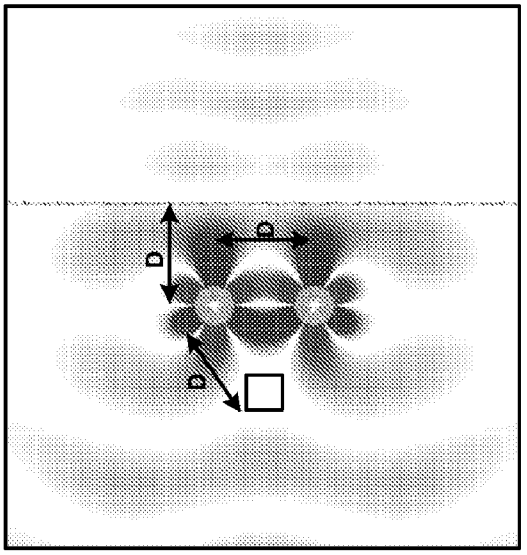
Disk with "human"	D_h/r	$Q_{c\text{-}h}^{abc}$	$Q_{c[h]}^{rad}$	$Q_{c[h]}$
Re{ε}=147.7, m=2	3	230	981	
$\lambda/r \approx 20$	5	2917	1984	
$Q_c^{abc} \approx 10096$	7	11573	2230	
	10	41496	2201	
Re{ε}=65.6, m=3	3	1827	6197	
$\lambda/r \approx 10$	**5**	**58431**	**11808**	
$Q_c^{abc} \approx 10096$	7	249748	9931	
	10	867552	9078	

FIG. 9A



Disk with "human"	D_w/r	$Q_{c\text{-}w}^{abc}$	$Q_{c[w]}^{rad}$	$Q_{c[w]}$
Re{ε}=147.7, m=2	3	16725	1235	1033
$\lambda/r \approx 20$	5	**31659**	**1922**	**1536**
$Q_c^{abc} \approx 10098$	7	49440	2389	1859
	10	82839	2140	1729
Re{ε}=65.6, m=3	3	53154	6228	3592
$\lambda/r \approx 10$	**5**	127402	10988	5053
$Q_c^{abc} \approx 10097$	7	159192	10168	4910
	10	191506	9510	4775

FIG. 9B



Two disks with "human" and "wall"	D/r	$Q_{c\text{-}h}^{abc}$	$Q_{c\text{-}w}^{abc}$	$Q_{c[hw]}^{rad}$	$Q_{w[hw]} = \omega/2\Gamma$	$\omega/2\kappa_{[hw]}$	$\kappa_{[hw]}/\Gamma_{c[hw]}$
Re{ε}=147.7, m=2	3	3300	12774	536	426	48	8.8
$\lambda/r \approx 20$	5	5719	26333	1600	1068	322	3.3
$Q_c^{abc} \approx 10100$	7	13248	50161	3542	2097	973	2.2
	10	18447	68460	3624	2254	1768	1.3
Re{ε}=65.6, m=3	3	2088	36661	6764	1328	141	9.4
$\lambda/r \approx 10$	**5**	**72137**	**90289**	**11945**	**4815**	**2114**	**2.3**
$Q_c^{abc} \approx 10100$	7	237822	129094	12261	5194	8307	0.6

FIG. 9C

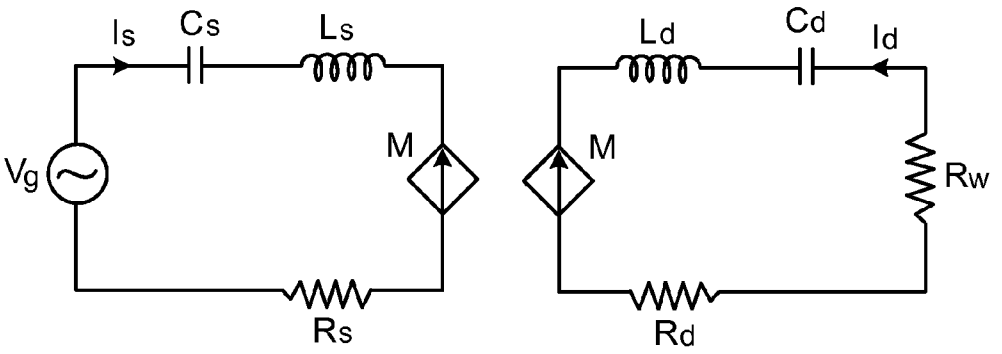

Is
Cs
Ls
Ld
Cd
Id
M
M
Vg
Rw
Rs
Rd

FIG. 10

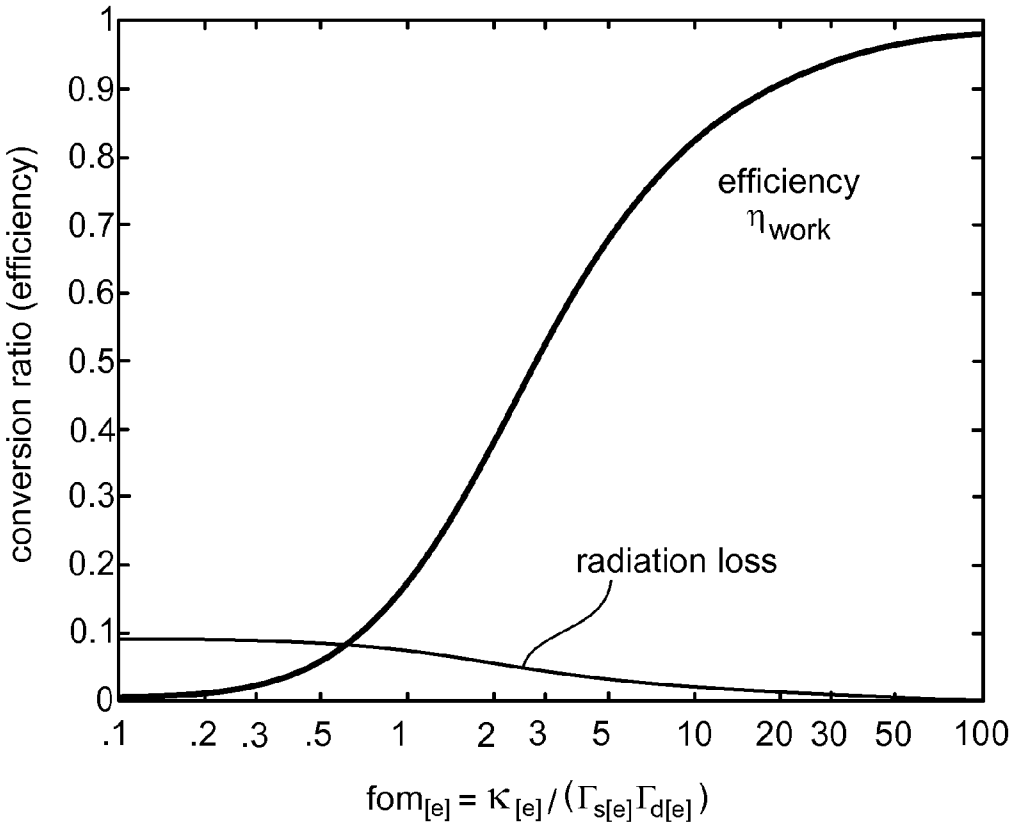
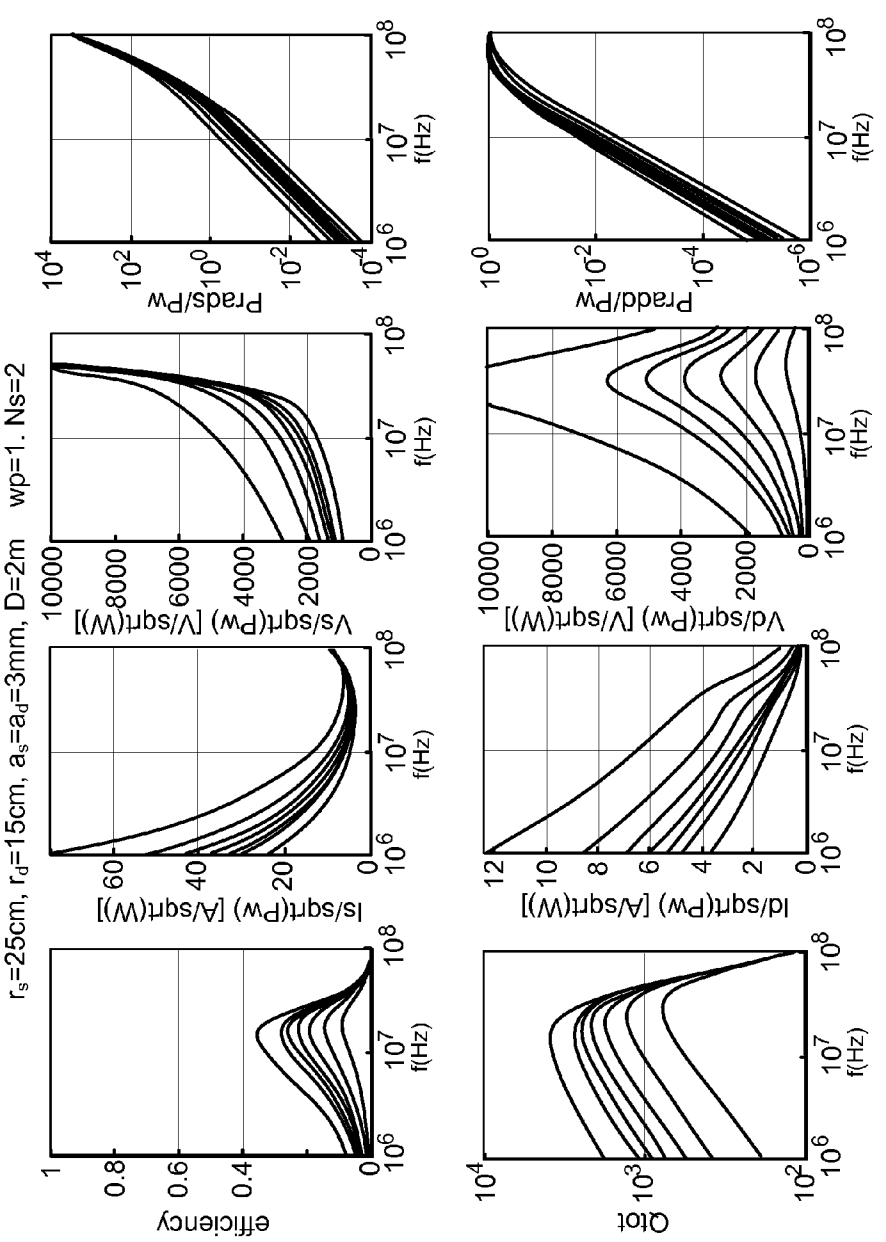
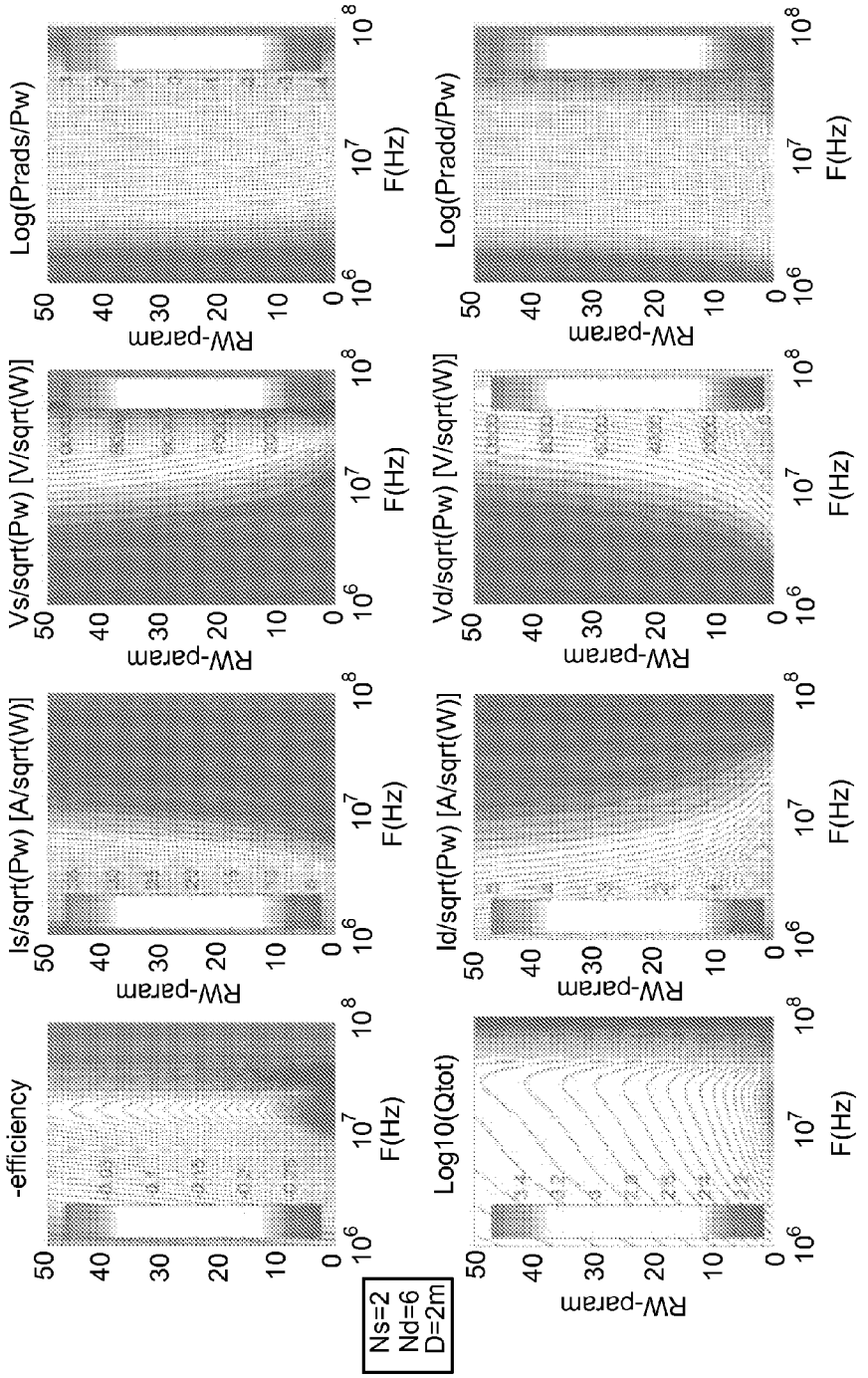

conversion ratio (efficiency)
efficiency
η_{work}
radiation loss
0
0.1
0.2
0.3
0.4
0.5
0.6
0.7
0.8
0.9
1
.1
.2
.3
.5
1
2
3
5
10
20
30
50
100
$fom_{[e]} = \kappa_{[e]} / (\Gamma_{s[e]} \Gamma_{d[e]})$

FIG. 11



Efficiency, total (loaded) device Q, and source and device currents, voltages and radiated powers , normalized to 1Watt of output working power, as functions of frequency for a particular choice of source and device loop dimensions, *wp* and N_s and different choices of N_d=1,2,3,4,5,6,10 (red, green, blue, magenta, yellow, cyan,. Black respectively)

FIG. 12



Efficiency, total (loaded device Q, and source and device currents, voltages and radiated powers (normalized to 1Watt of output working power) as functions of frequency and *wp* for a particular choice of source and device loop dimensions, and number of turns *Ns* and *Nd*.

FIG. 13

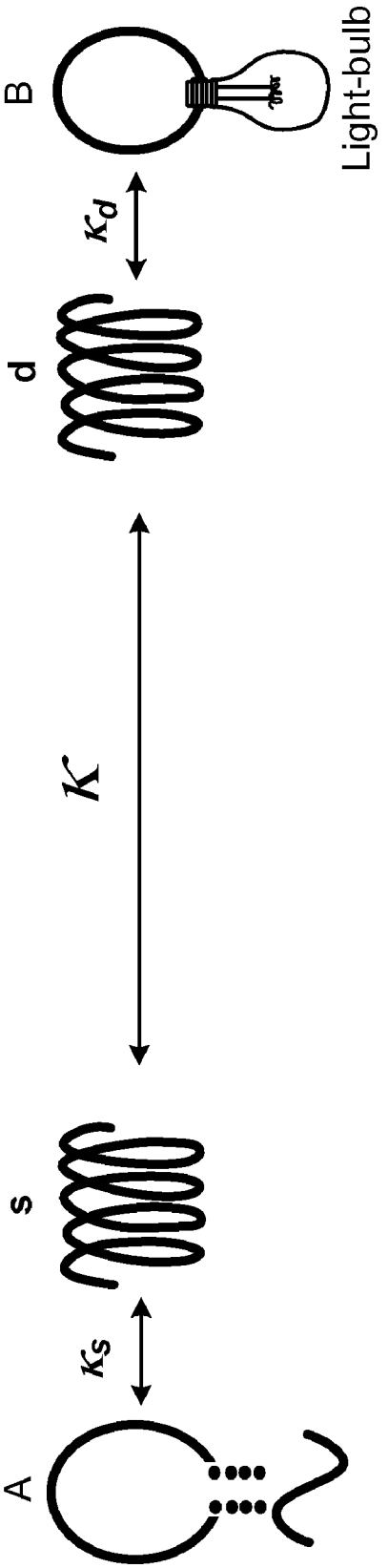
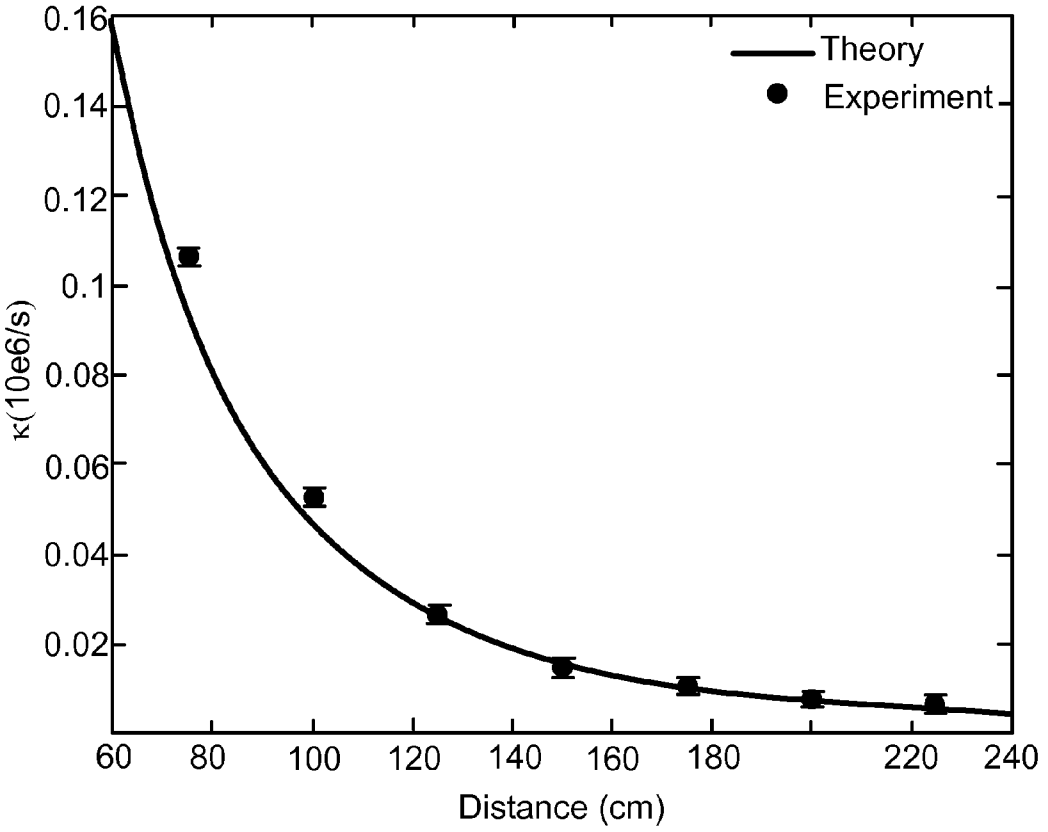
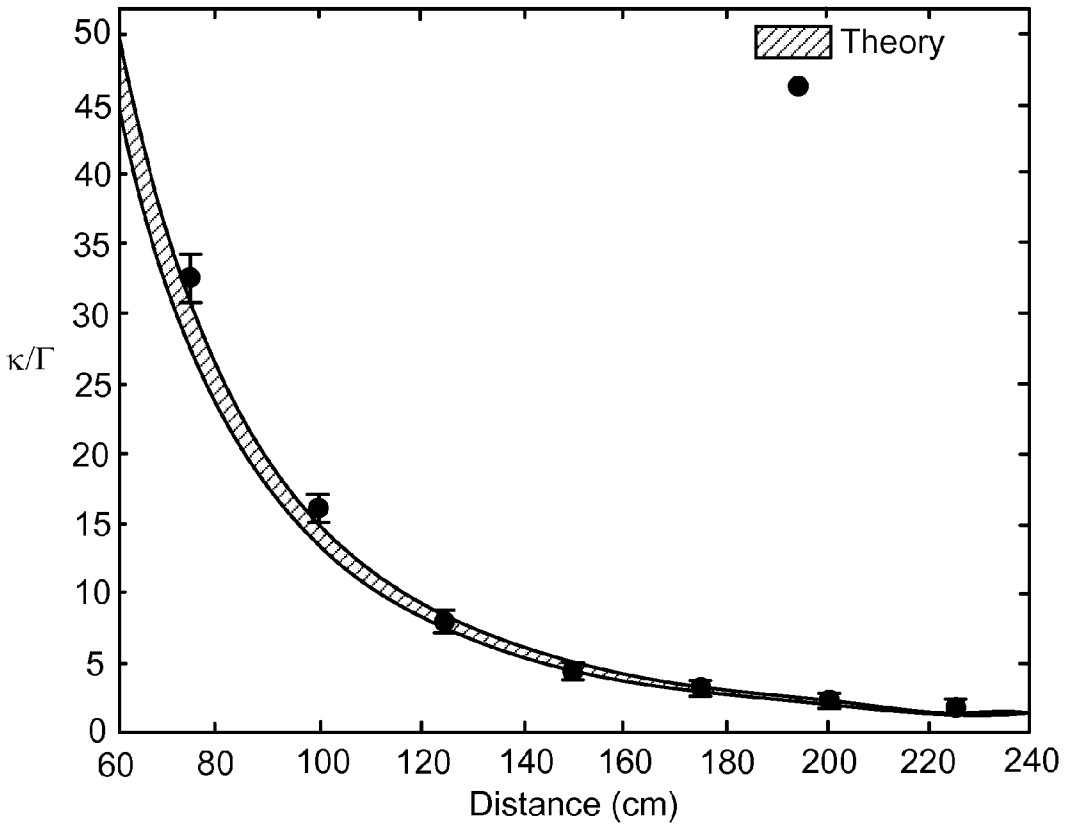


FIG. 14



Comparison of experimental and theoretical values for κ as a function of the separation between the source and device coils.

FIG. 15



Comparison of experimental and theoretical values for the parameter κ/Γ as a function of the separation between the two coils. The theory values are obtained by using the theoretically obtained κ and the experimentally measured Γ. The shaded area represents the spread in the theoretical κ/Γ due to the ~5% uncertainty in Q.

FIG.16

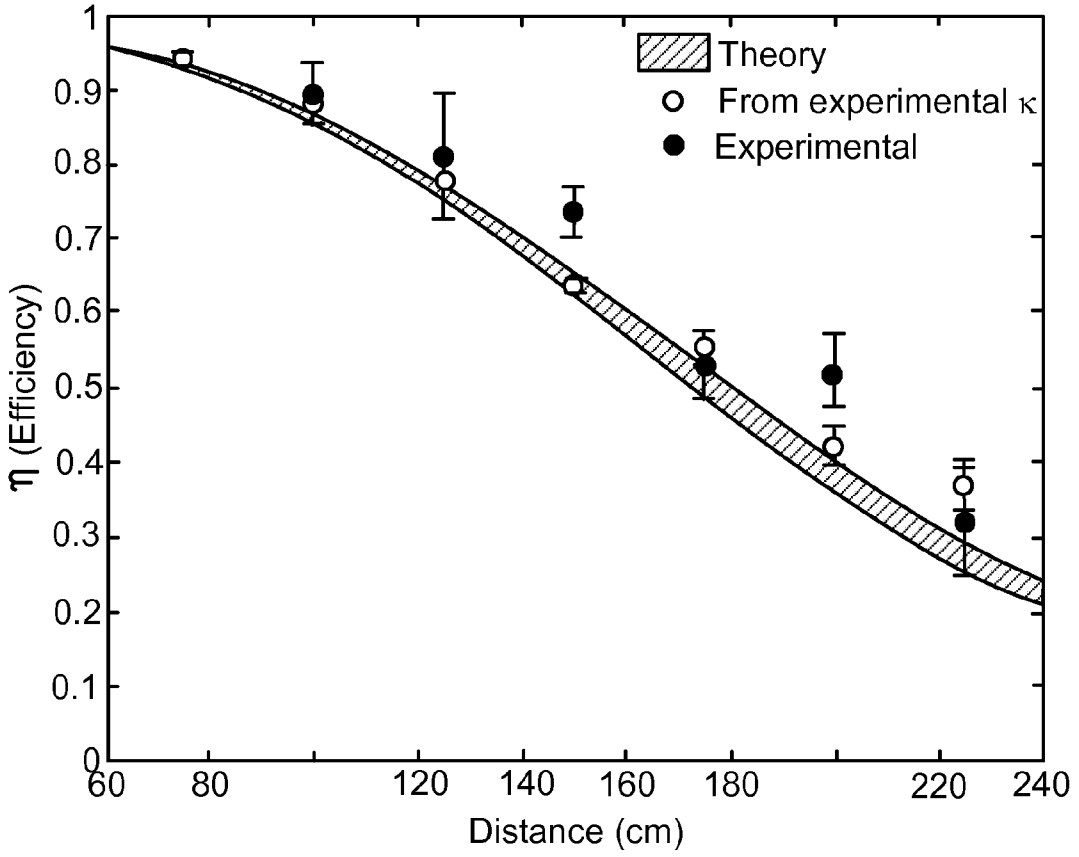

Theory
From experimental κ
Experimental
η (Efficiency)
Distance (cm)
0
0.1
0.2
0.3
0.4
0.5
0.6
0.7
0.8
0.9
1
60
80
120
140
160
180
220
240

FIG. 17

BIOLOGICAL EFFECTS OF MAGNETIC POWER TRANSFER

CROSS-REFERENCE TO RELATED APPLICATIONS

[0001] This application is a continuation of U.S. patent application Ser. No. 12/688,339 ('339 application) filed Jan. 15, 2010, the entirety of which is incorporated herein by reference. The '339 application is a continuation of U.S. patent application Ser. No. 12/055,963 ('963 Application), filed Mar. 26, 2008 the entirety of which is incorporated herein by reference. The '963 application claims the benefit of the following provisional applications, each of which is incorporated herein by reference in its entirety: U.S. Provisional Patent Application 60/908,383 filed Mar. 27, 2007; and U.S. Provisional Patent Application 60/908,666, filed Mar. 28, 2007.

[0002] The '963 application is a continuation-in-part of co-pending United States patent application entitled WIRELESS NON-RADIATIVE ENERGY TRANSFER filed on Jul. 5, 2006 and having Ser. No. 11/481,077 ('077 Application), the entirety of which is incorporated herein by reference. The '077 Application claims the benefit of provisional application Ser. No. 60/698,442 filed Jul. 12, 2005 ('442 Application), the entirety of which is incorporated herein by reference.

[0003] The '963 application, pursuant to U.S.C. §120 and U.S.C. §363, is a continuation-in-part of International Application No. PCT/US2007/070892, filed Jun. 11, 2007, which is incorporated herein by reference in its entirety, and which claims priority to the following provisional applications, each of which is incorporated herein by reference in its entirety: U.S. Provisional Patent Application 60/908,383 filed Mar. 27, 2007; and U.S. Provisional Patent Application 60/908,666, filed Mar. 28, 2007.

STATEMENT REGARDING GOVERNMENT FUNDING

[0004] This invention was made with government support awarded by the National Science Foundation under Grant No. DMR 02-13282. The government has certain rights in this invention.

BACKGROUND

[0005] The disclosure relates to wireless energy transfer. Wireless energy transfer may for example, be useful in such applications as providing power to autonomous electrical or electronic devices.

[0006] Radiative modes of omni-directional antennas (which work very well for information transfer) are not suitable for such energy transfer, because a vast majority of energy is wasted into free space. Directed radiation modes, using lasers or highly-directional antennas, can be efficiently used for energy transfer, even for long distances (transfer distance $L_{TRANS} \gg L_{DEV}$, where L_{DEV} is the characteristic size of the device and/or the source), but require existence of an uninterruptible line-of-sight and a complicated tracking system in the case of mobile objects. Some transfer schemes rely on induction, but are typically restricted to very close-range ($L_{TRANS} \ll L_{DEV}$) or low power (~mW) energy transfers.

[0007] The rapid development of autonomous electronics of recent years (e.g. laptops, cell-phones, house-hold robots, that all typically rely on chemical energy storage) has led to an increased need for wireless energy transfer.

SUMMARY

[0008] The inventors have realized that resonant objects with coupled resonant modes having localized evanescent field patterns may be used for non-radiative wireless energy transfer. Resonant objects tend to couple, while interacting weakly with other off-resonant environmental objects. Typically, using the techniques described below, as the coupling increases, so does the transfer efficiency. In some embodiments, using the below techniques, the energy-transfer rate can be larger than the energy-loss rate. Accordingly, efficient wireless energy-exchange can be achieved between the resonant objects, while suffering only modest transfer and dissipation of energy into other off-resonant objects. The nearly-omnidirectional but stationary (non-lossy) nature of the near field makes this mechanism suitable for mobile wireless receivers. Various embodiments therefore have a variety of possible applications including for example, placing a source (e.g. one connected to the wired electricity network) on the ceiling of a factory room, while devices (robots, vehicles, computers, or similar) are roaming freely within the room. Other applications include power supplies for electric-engine buses and/or hybrid cars and medical implantable devices.

[0009] In some embodiments, resonant modes are so-called magnetic resonances, for which most of the energy surrounding the resonant objects is stored in the magnetic field; i.e. there is very little electric field outside of the resonant objects. Since most everyday materials (including animals, plants and humans) are non-magnetic, their interaction with magnetic fields is minimal. This is important both for safety and also to reduce interaction with the extraneous environmental objects.

[0010] In one aspect, an apparatus is disclosed for use in wireless energy transfer, which includes a first resonator structure configured to transfer energy with a second resonator structure over a distance D greater than a characteristic size L_2 of the second resonator structure. In some embodiments, D is also greater than one or more of: a characteristic size L_1 of the first resonator structure, a characteristic thickness T_1 of the first resonator structure, and a characteristic width W_1 of the first resonator structure. The energy transfer is mediated by evanescent-tail coupling of a resonant field of the first resonator structure and a resonant field of the second resonator structure. The apparatus may include any of the following features alone or in combination.

[0011] In some embodiments, the first resonator structure is configured to transfer energy to the second resonator structure. In some embodiments, the first resonator structure is configured to receive energy from the second resonator structure. In some embodiments, the apparatus includes the second resonator structure.

[0012] In some embodiments, the first resonator structure has a resonant angular frequency ω_1, a Q-factor Q_1, and a resonance width Γ_1, the second resonator structure has a resonant angular frequency ω_2, a Q-factor Q_2, and a resonance width Γ_2, and the energy transfer has a rate κ. In some embodiments, the absolute value of the difference of the angular frequencies ω_1 and ω_2 is smaller than the broader of the resonant widths Γ_1 and Γ_2.

[0013] In some embodiments $Q_1>100$ and $Q_2>100$, $Q_1>300$ and $Q_2>300$, $Q_1>500$ and $Q_2>500$, or $Q_1>1000$ and

Q_2>1000. In some embodiments, Q_1>100 or Q_2>100, Q_1>300 or Q_2>300, Q_1>500 or Q_2>500, or Q_1>1000 or Q_2>1000.

[0014] In some embodiments, the coupling to loss ratio

$$\frac{\kappa}{\sqrt{\Gamma_1\Gamma_2}} > 0.5,\ \frac{\kappa}{\sqrt{\Gamma_1\Gamma_2}} > 1,\ \frac{\kappa}{\sqrt{\Gamma_1\Gamma_2}} > 2,\ \text{or}\ \frac{\kappa}{\sqrt{\Gamma_1\Gamma_2}} > 5.$$

In some such embodiments, D/L_2 may be as large as 2, as large as 3, as large as 5, as large as 7, or as large as 10.

[0015] In some embodiments, Q_1>1000 and Q_2>1000, and the coupling to loss ratio

$$\frac{\kappa}{\sqrt{\Gamma_1\Gamma_2}} > 10,\ \frac{\kappa}{\sqrt{\Gamma_1\Gamma_2}} > 25,\ \text{or}\ \frac{\kappa}{\sqrt{\Gamma_1\Gamma_2}} > 40.$$

In some such embodiments, D/L_2 may be as large as 2, as large as 3, as large as 5, as large as 7, as large as 10.

[0016] In some embodiments, $Q_\kappa=\omega/2\kappa$ is less than about 50, less than about 200, less than about 500, or less than about 1000. In some such embodiments, D/L_2 is as large as 2, as large as 3, as large as 5, as large as 7, or as large as 10.

[0017] In some embodiments, the quantity $\kappa/\sqrt{\Gamma_1\theta_2}$ is maximized at an angular frequency ω with a frequency width Ғ around the maximum, and the absolute value of the difference of the angular frequencies ω_1 and ω is smaller than the width θ, and the absolute value of the difference of the angular frequencies ω_2 and ω is smaller than the width Ғ.

[0018] In some embodiments, the energy transfer operates with an efficiency η_{work} greater than about 1%, greater than about 10%, greater than about 30%, greater than about 50%, or greater than about 80%.

[0019] In some embodiments, the energy transfer operates with a radiation loss η_{rad} less that about 10%. In some such embodiments the coupling to loss ratio

$$\frac{\kappa}{\sqrt{\Gamma_1\Gamma_2}} \geq 0.1.$$

[0020] In some embodiments, the energy transfer operates with a radiation loss η_{rad} less that about 1%. In some such embodiments, the coupling to loss ratio

$$\frac{\kappa}{\sqrt{\Gamma_1\Gamma_2}} \geq 1.$$

[0021] In some embodiments, in the presence of a human at distance of more than 3 cm from the surface of either resonant object, the energy transfer operates with a loss to the human η_κ of less than about 1%. In some such embodiments the coupling to loss ratio

$$\frac{\kappa}{\sqrt{\Gamma_1\Gamma_2}} \geq 1.$$

[0022] In some embodiments, in the presence of a human at distance of more than 10 cm from the surface of either resonant object, the energy transfer operates with a loss to the human η_κ of less than about 0.2%. In some such embodiments the coupling to loss ratio

$$\frac{\kappa}{\sqrt{\Gamma_1\Gamma_2}} \geq 1.$$

[0023] In some embodiments, during operation, a device coupled to the first or second resonator structure with a coupling rate Γ_{work} receives a usable power P_{work} from the resonator structure.

[0024] In some embodiments, P_{work} is greater than about 0.01 Watt, greater than about 0.1 Watt, greater than about 1 Watt, or greater than about 10 Watt.

[0025] In some embodiments, if the device is coupled to the first resonator, then $\frac{1}{2} \leqq [(\Gamma_{work}/\Gamma_1)^2-1]/(\kappa/\sqrt{\Gamma_1\Gamma_2})^2 \leqq 2$, or $\frac{1}{4} \leqq [(\Gamma_{work}/\Gamma_1)^2-1]/(\kappa/\sqrt{\Gamma_1\Gamma_2})^2 \leqq 4$, or $\frac{1}{8} \leqq [(\Gamma_{work}/\Gamma_1)^2-1]/(\kappa/\sqrt{\Gamma_1\Gamma_2})^2 \leqq 8$, and, if the device is coupled to the second resonator, then $\frac{1}{2} \leqq [(\Gamma_{work}/\Gamma_2)^2-1]/(\kappa/\sqrt{\Gamma_1\Gamma_2})^2 \leqq 2$, or $\frac{1}{4} \leqq [(\Gamma_{work}/\Gamma_2)^2 1]/(\kappa/\sqrt{\Gamma_1\Gamma_2})^2 \leqq 4$, or $\frac{1}{8} \leqq [(\Gamma_{work}/\Gamma_2)^2-1]/(\kappa/\sqrt{\Gamma_1\Gamma_2})^2 \leqq 8$.

[0026] In some embodiments, the device includes an electrical or electronic device. In some embodiments, the device includes a robot (e.g. a conventional robot or a nano-robot). In some embodiments, the device includes a mobile electronic device (e.g. a telephone, or a cell-phone, or a computer, or a laptop computer, or a personal digital assistant (PDA)). In some embodiments, the device includes an electronic device that receives information wirelessly (e.g. a wireless keyboard, or a wireless mouse, or a wireless computer screen, or a wireless television screen). In some embodiments, the device includes a medical device configured to be implanted in a patient (e.g. an artificial organ, or implant configured to deliver medicine). In some embodiments, the device includes a sensor. In some embodiments, the device includes a vehicle (e.g. a transportation vehicle, or an autonomous vehicle).

[0027] In some embodiments, the apparatus further includes the device.

[0028] In some embodiments, during operation, a power supply coupled to the first or second resonator structure with a coupling rate Γ_{supply} drives the resonator structure at a frequency f and supplies power P_{total}. In some embodiments, the absolute value of the difference of the angular frequencies $\omega=2\pi f$ and ω_1 is smaller than the resonant width Γ_1, and the absolute value of the difference of the angular frequencies $\omega=2\pi f$ and ω_2 is smaller than the resonant width Γ_2. In some embodiments, f is about the optimum efficiency frequency.

[0029] In some embodiments, if the power supply is coupled to the first resonator, then $\frac{1}{2} \leqq [(\Gamma_{supply}/\Gamma_1)^2-1]/(\kappa/\sqrt{\Gamma_1\Gamma_2})^2 \leqq 2$, or $\frac{1}{4} \leqq [(\Gamma_{supply}/\Gamma_1)_2-1]/(\kappa/\sqrt{\Gamma_1\Gamma_2})^2 \leqq 4$, or $\frac{1}{8} \leqq [(\Gamma_{supply}/\Gamma_1)^2-1]/(\kappa/\sqrt{\Gamma_1\Gamma_2})^2 \leqq 8$, and, if the power supply is coupled to the second resonator, then $\frac{1}{2} \leqq [(\Gamma_{supply}/\Gamma_2)^2-1]/(\kappa/\sqrt{\Gamma_1\Gamma_2})^2 \leqq 2$, or $\frac{1}{4} \leqq [(\Gamma_{supply}/\Gamma_2)^2-1]/(\kappa/\sqrt{\Gamma_1\Gamma_2})^2 \leqq 4$, or $\frac{1}{8} \leqq [(\Gamma_{supply}/\Gamma_2)^2-1]/(\kappa/\sqrt{\Gamma_1\Gamma_2})^2 \leqq 8$.

[0030] In some embodiments, the apparatus further includes the power source.

[0031] In some embodiments, the resonant fields are electromagnetic. In some embodiments, f is about 50 GHz or less, about 1 GHz or less, about 100 MHz or less, about 10 MHz or less, about 1 MHz or less, about 100 KHz or less, or about 10 kHz or less. In some embodiments, f is about 50 GHz or greater, about 1 GHz or greater, about 100 MHz or greater,

about 10 MHz or greater, about 1 MHz or greater, about 100 kHz or greater, or about 10 kHz or greater. In some embodiments, f is within one of the frequency bands specially assigned for industrial, scientific and medical (ISM) equipment.

[0032] In some embodiments, the resonant fields are primarily magnetic in the area outside of the resonant objects. In some such embodiments, the ratio of the average electric field energy to average magnetic filed energy at a distance D_p from the closest resonant object is less than 0.01, or less than 0.1. In some embodiments, L_R is the characteristic size of the closest resonant object and D_p/L_R is less than 1.5, 3, 5, 7, or 10.

[0033] In some embodiments, the resonant fields are acoustic. In some embodiments, one or more of the resonant fields include a whispering gallery mode of one of the resonant structures.

[0034] In some embodiments, one of the first and second resonator structures includes a self resonant coil of conducting wire, conducting Litz wire, or conducting ribbon. In some embodiments, both of the first and second resonator structures include self resonant coils of conducting wire, conducting Litz wire, or conducting ribbon. In some embodiments, both of the first and second resonator structures include self resonant coils of conducting wire or conducting Litz wire or conducting ribbon, and $Q_1>300$ and $Q_2>300$.

[0035] In some embodiments, one or more of the self resonant conductive wire coils include a wire of length/and cross section radius a wound into a helical coil of radius r, height h and number of turns N. In some embodiments, $N=\sqrt{l^2-h^2}/2\pi r$.

[0036] In some embodiments, for each resonant structure r is about 30 cm, h is about 20 cm, a is about 3 mm and N is about 5.25, and, during operation, a power source coupled to the first or second resonator structure drives the resonator structure at a frequency f. In some embodiments, f is about 10.6 MHz. In some such embodiments, the coupling to loss ratio

$$\frac{\kappa}{\sqrt{\Gamma_1\Gamma_2}} \geq 40, \frac{\kappa}{\sqrt{\Gamma_1\Gamma_2}} \geq 15, \text{ or } \frac{\kappa}{\sqrt{\Gamma_1\Gamma_2}} \geq 5, \text{ or } \frac{\kappa}{\sqrt{\Gamma_1\Gamma_2}} \geq 1.$$

In some such embodiments D/L_R is as large as about 2, 3, 5, or 8.

[0037] In some embodiments, for each resonant structure r is about 30 cm, h is about 20 cm, a is about 1 cm and N is about 4, and, during operation, a power source coupled to the first or second resonator structure drives the resonator structure at a frequency f. In some embodiments, f is about 13.4 MHz. In some such embodiments, the coupling to loss ratio

$$\frac{\kappa}{\sqrt{\Gamma_1\Gamma_2}} \geq 70, \frac{\kappa}{\sqrt{\Gamma_1\Gamma_2}} \geq 19, \text{ or } \frac{\kappa}{\sqrt{\Gamma_1\Gamma_2}} \geq 8, \text{ or } \frac{\kappa}{\sqrt{\Gamma_1\Gamma_2}} \geq 3.$$

In some such embodiments D/L_R is as large as about 3, 5, 7, or 10.

[0038] In some embodiments, for each resonant structure r is about 10 cm, h is about 3 cm, a is about 2 mm and N is about 6, and, during operation, a power source coupled to the first or second resonator structure drives the resonator structure at a frequency f. In some embodiments, f is about 21.4 MHz. In some such embodiments, the coupling to loss ratio

$$\frac{\kappa}{\sqrt{\Gamma_1\Gamma_2}} \geq 59, \frac{\kappa}{\sqrt{\Gamma_1\Gamma_2}} \geq 15, \text{ or } \frac{\kappa}{\sqrt{\Gamma_1\Gamma_2}} \geq 6, \text{ or } \frac{\kappa}{\sqrt{\Gamma_1\Gamma_2}} \geq 2.$$

In some such embodiments D/L_R is as large as about 3, 5, 7, or 10.

[0039] In some embodiments, one of the first and second resonator structures includes a capacitively loaded loop or coil of conducting wire, conducting Litz wire, or conducting ribbon. In some embodiments, both of the first and second resonator structures include capacitively loaded loops or coils of conducting wire, conducting Litz wire, or conducting ribbon. In some embodiments, both of the first and second resonator structures include capacitively loaded loops or coils of conducting wire or conducting Litz wire or conducting ribbon, and $Q_1>300$ and $Q_2>300$.

[0040] In some embodiments, the characteristic size L_R of the resonator structure receiving energy from the other resonator structure is less than about 1 cm and the width of the conducting wire or Litz wire or ribbon of said object is less than about 1 mm, and, during operation, a power source coupled to the first or second resonator structure drives the resonator structure at a frequency f. In some embodiments, f is about 380 MHz. In some such embodiments, the coupling to loss ratio

$$\frac{\kappa}{\sqrt{\Gamma_1\Gamma_2}} \geq 14.9, \frac{\kappa}{\sqrt{\Gamma_1\Gamma_2}} \geq 3.2, \frac{\kappa}{\sqrt{\Gamma_1\Gamma_2}} \geq 1.2, \text{ or } \frac{\kappa}{\sqrt{\Gamma_1\Gamma_2}} \geq 0.4.$$

In some such embodiments, D/L_R is as large as about 3, about 5, about 7, or about 10.

[0041] In some embodiments, the characteristic size of the resonator structure receiving energy from the other resonator structure L_R is less than about 10 cm and the width of the conducting wire or Litz wire or ribbon of said object is less than about 1 cm, and, during operation, a power source coupled to the first or second resonator structure drives the resonator structure at a frequency f. In some embodiments, f is about 43 MHz. In some such embodiments, the coupling to loss ratio

$$\frac{\kappa}{\sqrt{\Gamma_1\Gamma_2}} \geq 15.9, \frac{\kappa}{\sqrt{\Gamma_1\Gamma_2}} \geq 4.3, \frac{\kappa}{\sqrt{\Gamma_1\Gamma_2}} \geq 1.8, \text{ or } \frac{\kappa}{\sqrt{\Gamma_1\Gamma_2}} \geq 0.7.$$

In some such embodiments, D/L_R, is as large as about 3, about 5, about 7, or about 10.

[0042] In some embodiments, the characteristic size L_R, of the resonator structure receiving energy from the other resonator structure is less than about 30 cm and the width of the conducting wire or Litz wire or ribbon of said object is less than about 5 cm, and, during operation, a power source coupled to the first or second resonator structure drives the resonator structure at a frequency f. In some such embodiments, f is about 9 MHz. In some such embodiments, the coupling to loss ratio

$$\frac{\kappa}{\sqrt{\Gamma_1\Gamma_2}} \geq 67.4, \frac{\kappa}{\sqrt{\Gamma_1\Gamma_2}} \geq 17.8, \frac{\kappa}{\sqrt{\Gamma_1\Gamma_2}} \geq 7.1, \text{ or } \frac{\kappa}{\sqrt{\Gamma_1\Gamma_2}} \geq 2.7.$$

In some such embodiments, D/L_R, is as large as about 3, about 5, about 7, or about 10.

[0043] In some embodiments, the characteristic size of the resonator structure receiving energy from the other resonator structure L_R, is less than about 30 cm and the width of the conducting wire or Litz wire or ribbon of said object is less than about 5 mm, and, during operation, a power source coupled to the first or second resonator structure drives the resonator structure at a frequency f. In some embodiments, f is about 17 MHz. In some such embodiments, the coupling to loss ratio

$$\frac{\kappa}{\sqrt{\Gamma_1\Gamma_2}} \geq 6.3, \frac{\kappa}{\sqrt{\Gamma_1\Gamma_2}} \geq 1.3, \frac{\kappa}{\sqrt{\Gamma_1\Gamma_2}} \geq 0.5., \text{ or } \frac{\kappa}{\sqrt{\Gamma_1\Gamma_2}} \geq 0.2.$$

In some such embodiments, D/L_R is as large as about 3, about 5, about 7, or about 10.

[0044] In some embodiments, the characteristic size L_R of the resonator structure receiving energy from the other resonator structure is less than about 1 m, and the width of the conducting wire or Litz wire or ribbon of said object is less than about 1 cm, and, during operation, a power source coupled to the first or second resonator structure drives the resonator structure at a frequency f. In some embodiments, f is about 5 MHz. In some such embodiments, the coupling to loss ratio

$$\frac{\kappa}{\sqrt{\Gamma_1\Gamma_2}} \geq 6.8, \frac{\kappa}{\sqrt{\Gamma_1\Gamma_2}} \geq 1.4, \frac{\kappa}{\sqrt{\Gamma_1\Gamma_2}} \geq 0.5, \frac{\kappa}{\sqrt{\Gamma_1\Gamma_2}} \geq 0.2.$$

In some such embodiments, D/L_R is as large as about 3, about 5, about 7, or about 10.

[0045] In some embodiments, during operation, one of the resonator structures receives a usable power P_w from the other resonator structure, an electrical current I_s flows in the resonator structure which is transferring energy to the other resonant structure, and the ratio

$$\frac{I_s}{\sqrt{P_w}}$$

is less than about 5 Amps/$\sqrt{\text{Watts}}$ or less than about 2 Amps/$\sqrt{\text{Watts}}$. In some embodiments, during operation, one of the resonator structures receives a usable power P_w from the other resonator structure, a voltage difference V_s appears across the capacitive element of the first resonator structure, and the ratio

$$\frac{V_s}{\sqrt{P_w}}$$

is less than about 2000 Volts/$\sqrt{\text{Watts}}$ or less than about 4000 Volts/$\sqrt{\text{Watts}}$.

[0046] In some embodiments, one of the first and second resonator structures includes a inductively loaded rod of conducting wire or conducting Litz wire or conducting ribbon. In some embodiments, both of the first and second resonator structures include inductively loaded rods of conducting wire or conducting Litz wire or conducting ribbon. In some embodiments, both of the first and second resonator structures include inductively loaded rods of conducting wire or conducting Litz wire or conducting ribbon, and $Q_1>300$ and $Q_2>300$.

[0047] In some embodiments, the characteristic size of the resonator structure receiving energy from the other resonator structure L_R is less than about 10 cm and the width of the conducting wire or Litz wire or ribbon of said object is less than about 1 cm, and, during operation, a power source coupled to the first or second resonator structure drives the resonator structure at a frequency f. In some embodiments, f is about 14 MHz. In some such embodiments, the coupling to loss ratio

$$\frac{\kappa}{\sqrt{\Gamma_1\Gamma_2}} \geq 32, \frac{\kappa}{\sqrt{\Gamma_1\Gamma_2}} \geq 5.8, \frac{\kappa}{\sqrt{\Gamma_1\Gamma_2}} \geq 2, \text{ or } \frac{\kappa}{\sqrt{\Gamma_1\Gamma_2}} \geq 0.6.$$

In some such embodiments, D/L_R is as large as about 3, about 5, about 7, or about 10.

[0048] In some embodiments, the characteristic size L_R of the resonator structure receiving energy from the other resonator structure is less than about 30 cm and the width of the conducting wire or Litz wire or ribbon of said object is less than about 5 cm, and, during operation, a power source coupled to the first or second resonator structure drives the resonator structure at a frequency f. In some such embodiments, f is about 2.5 MHz. In some such embodiments, the coupling to loss ratio

$$\frac{\kappa}{\sqrt{\Gamma_1\Gamma_2}} \geq 105, \frac{\kappa}{\sqrt{\Gamma_1\Gamma_2}} \geq 19, \frac{\kappa}{\sqrt{\Gamma_1\Gamma_2}} \geq 6.6, \text{ or } \frac{\kappa}{\sqrt{\Gamma_1\Gamma_2}} \geq 2.2.$$

In some such embodiments, D/L_R is as large as about 3, about 5, about 7, or about 10.

[0049] In some embodiments, one of the first and second resonator structures includes a dielectric disk. In some embodiments, both of the first and second resonator structures include dielectric disks. In some embodiments, both of the first and second resonator structures include dielectric disks, and $Q_1>300$ and $Q_2>300$.

[0050] In some embodiments, the characteristic size of the resonator structure receiving energy from the other resonator structure is L_R and the real part of the permittivity of said resonator structure $\in$ is less than about 150. In some such embodiments, the coupling to loss ratio

$$\frac{\kappa}{\sqrt{\Gamma_1\Gamma_2}} \geq 42.4, \frac{\kappa}{\sqrt{\Gamma_1\Gamma_2}} \geq 6.5, \frac{\kappa}{\sqrt{\Gamma_1\Gamma_2}} \geq 2.3, \frac{\kappa}{\sqrt{\Gamma_1\Gamma_2}} \geq 0.5.$$

In some such embodiments, D/L_R is as large as about 3, about 5, about 7, or about 10.

[0051] In some embodiments, the characteristic size of the resonator structure receiving energy from the other resonator structure is L_R and the real part of the permittivity of said resonator structure $\in$ is less than about 65. In some such embodiments, the coupling to loss ratio

$$\frac{\kappa}{\sqrt{\Gamma_1\Gamma_2}} \geq 30.9, \frac{\kappa}{\sqrt{\Gamma_1\Gamma_2}} \geq 2.3, \text{ or } \frac{\kappa}{\sqrt{\Gamma_1\Gamma_2}} \geq 0.5.$$

In some such embodiments, D/L_R is as large as about 3, about 5, about 7.

[0052] In some embodiments, at least one of the first and second resonator structures includes one of: a dielectric material, a metallic material, a metallodielectric object, a plasmonic material, a plasmonodielectric object, a superconducting material.

[0053] In some embodiments, at least one of the resonators has a quality factor greater than about 5000, or greater than about 10000.

[0054] In some embodiments, the apparatus also includes a third resonator structure configured to transfer energy with one or more of the first and second resonator structures, where the energy transfer between the third resonator structure and the one or more of the first and second resonator structures is mediated by evanescent-tail coupling of the resonant field of the one or more of the first and second resonator structures and a resonant field of the third resonator structure.

[0055] In some embodiments, the third resonator structure is configured to transfer energy to one or more of the first and second resonator structures.

[0056] In some embodiments, the first resonator structure is configured to receive energy from one or more of the first and second resonator structures.

[0057] In some embodiments, the first resonator structure is configured to receive energy from one of the first and second resonator structures and transfer energy to the other one of the first and second resonator structures.

[0058] Some embodiments include a mechanism for, during operation, maintaining the resonant frequency of one or more of the resonant objects. In some embodiments, the feedback mechanism comprises an oscillator with a fixed frequency and is configured to adjust the resonant frequency of the one or more resonant objects to be about equal to the fixed frequency. In some embodiments, the feedback mechanism is configured to monitor an efficiency of the energy transfer, and adjust the resonant frequency of the one or more resonant objects to maximize the efficiency.

[0059] In another aspect, a method of wireless energy transfer is disclosed, which method includes providing a first resonator structure and transferring energy with a second resonator structure over a distance D greater than a characteristic size L_2 of the second resonator structure. In some embodiments, D is also greater than one or more of: a characteristic size L_1 of the first resonator structure, a characteristic thickness T_1 of the first resonator structure, and a characteristic width W_1 of the first resonator structure. The energy transfer is mediated by evanescent-tail coupling of a resonant field of the first resonator structure and a resonant field of the second resonator structure.

[0060] In some embodiments, the first resonator structure is configured to transfer energy to the second resonator structure. In some embodiments, the first resonator structure is configured to receive energy from the second resonator structure.

[0061] In some embodiments, the first resonator structure has a resonant angular frequency ω_1, a Q-factor Q_1, and a resonance width Γ_1, the second resonator structure has a resonant angular frequency ω_2, a Q-factor Q_2, and a resonance width Γ_2, and the energy transfer has a rate κ. In some embodiments, the absolute value of the difference of the angular frequencies ω_1 and ω_2 is smaller than the broader of the resonant widths Γ_1 and Γ_2.

[0062] In some embodiments, the coupling to loss ratio

$$\frac{\kappa}{\sqrt{\Gamma_1\Gamma_2}} > 0.5, \frac{\kappa}{\sqrt{\Gamma_1\Gamma_2}} > 1, \frac{\kappa}{\sqrt{\Gamma_1\Gamma_2}} > 2, \text{ or } \frac{\kappa}{\sqrt{\Gamma_1\Gamma_2}} > 5.$$

In some such embodiments, D/L_2 may be as large as 2, as large as 3, as large as 5, as large as 7, or as large as 10.

[0063] In another aspect, an apparatus is disclosed for use in wireless information transfer which includes a first resonator structure configured to transfer information by transferring energy with a second resonator structure over a distance D greater than a characteristic size L_2 of the second resonator structure. In some embodiments, D is also greater than one or more of: a characteristic size L_1 of the first resonator structure, a characteristic thickness T_1 of the first resonator structure, and a characteristic width W_1 of the first resonator structure. The energy transfer is mediated by evanescent-tail coupling of a resonant field of the first resonator structure and a resonant field of the second resonator structure.

[0064] In some embodiments, the first resonator structure is configured to transfer energy to the second resonator structure. In some embodiments, the first resonator structure is configured to receive energy from the second resonator structure. In some embodiments the apparatus includes, the second resonator structure.

[0065] In some embodiments, the first resonator structure has a resonant angular frequency ω_1, a Q-factor Q_1, and a resonance width Γ_1, the second resonator structure has a resonant angular frequency ω_2, a Q-factor Q_2, and a resonance width Γ_2, and the energy transfer has a rate κ. In some embodiments, the absolute value of the difference of the angular frequencies $\int_1$ and ω_2 is smaller than the broader of the resonant widths Γ_1 and Γ_2.

[0066] In some embodiments, the coupling to loss ratio

$$\frac{\kappa}{\sqrt{\Gamma_1\Gamma_2}} > 0.5, \frac{\kappa}{\sqrt{\Gamma_1\Gamma_2}} > 1, \frac{\kappa}{\sqrt{\Gamma_1\Gamma_2}} > 2, \text{ or } \frac{\kappa}{\sqrt{\Gamma_1\Gamma_2}} > 5.$$

In some such embodiments, D/L_2 may be as large as 2, as large as 3, as large as 5, as large as 7, or as large as 10.

[0067] In another aspect, a method of wireless information transfer is disclosed, which method includes providing a first resonator structure and transferring information by transferring energy with a second resonator structure over a distance

D greater than a characteristic size L_2 of the second resonator structure. In some embodiments, D is also greater than one or more of: a characteristic size L_1 of the first resonator structure, a characteristic thickness T_1 of the first resonator structure, and a characteristic width W_1 of the first resonator structure. The energy transfer is mediated by evanescent-tail coupling of a resonant field of the first resonator structure and a resonant field of the second resonator structure.

[0068] In some embodiments, the first resonator structure is configured to transfer energy to the second resonator structure. In some embodiments, the first resonator structure is configured to receive energy from the second resonator structure.

[0069] In some embodiments, the first resonator structure has a resonant angular frequency ω_1, a Q-factor Q_1, and a resonance width Γ_1, the second resonator structure has a resonant angular frequency κ, a Q-factor Q_2, and a resonance width Γ_2, and the energy transfer has a rate κ. In some embodiments, the absolute value of the difference of the angular frequencies and κ_2 is smaller than the broader of the resonant widths Γ_1 and Γ_2.

[0070] In some embodiments, the coupling to loss ratio

$$\frac{\kappa}{\sqrt{\Gamma_1\Gamma_2}} > 0.5, \frac{\kappa}{\sqrt{\Gamma_1\Gamma_2}} > 1, \frac{\kappa}{\sqrt{\Gamma_1\Gamma_2}} > 2, \text{ or } \frac{\kappa}{\sqrt{\Gamma_1\Gamma_2}} > 5.$$

In some such embodiments, D/L_2 may be as large as 2, as large as 3, as large as 5, as large as 7, or as large as 10.

[0071] It is to be understood that the characteristic size of an object is equal to the radius of the smallest sphere which can fit around the entire object. The characteristic thickness of an object is, when placed on a flat surface in any arbitrary configuration, the smallest possible height of the highest point of the object above a flat surface. The characteristic width of an object is the radius of the smallest possible circle that the object can pass through while traveling in a straight line. For example, the characteristic width of a cylindrical object is the radius of the cylinder.

[0072] The distance D over which the energy transfer between two resonant objects occurs is the distance between the respective centers of the smallest spheres which can fit around the entirety of each object. However, when considering the distance between a human and a resonant object, the distance is to be measured from the outer surface of the human to the outer surface of the sphere.

[0073] As described in detail below, non-radiative energy transfer refers to energy transfer effected primarily through the localized near field, and, at most, secondarily through the radiative portion of the field.

[0074] It is to be understood that an evanescent tail of a resonant object is the decaying non-radiative portion of a resonant field localized at the object. The decay may take any functional form including, for example, an exponential decay or power law decay.

[0075] The optimum efficiency frequency of a wireless energy transfer system is the frequency at which the figure of merit

$$\frac{\kappa}{\sqrt{\Gamma_1\Gamma_2}}$$

is maximized, all other factors held constant.

[0076] The resonant width (Γ) refers to the width of an object's resonance due to object's intrinsic losses (e.g. loss to absorption, radiation, etc.).

[0077] It is to be understood that a Q-factor (Q) is a factor that compares the time constant for decay of an oscillating system's amplitude to its oscillation period. For a given resonator mode with angular frequency ω and resonant width Γ, the Q-factor $Q=\omega/2\Gamma$.

[0078] The energy transfer rate (κ) refers to the rate of energy transfer from one resonator to another. In the coupled mode description described below it is the coupling constant between the resonators.

[0079] It is to be understood that $Q_\kappa=\omega/2\kappa$.

[0080] Unless otherwise defined, all technical and scientific terms used herein have the same meaning as commonly understood by one of ordinary skill in the art to which this invention belongs. In case of conflict with publications, patent applications, patents, and other references mentioned incorporated herein by reference, the present specification, including definitions, will control.

[0081] Various embodiments may include any of the above features, alone or in combination. Other features, objects, and advantages of the disclosure will be apparent from the following detailed description.

[0082] Other features, objects, and advantages of the disclosure will be apparent from the following detailed description.

BRIEF DESCRIPTION OF THE DRAWINGS

[0083] FIG. **1** shows a schematic of a wireless energy transfer scheme.

[0084] FIG. **2** shows an example of a self-resonant conducting-wire coil.

[0085] FIG. **3** shows a wireless energy transfer scheme featuring two self-resonant conducting-wire coils

[0086] FIG. **4** shows an example of a capacitively loaded conducting-wire coil, and illustrates the surrounding field.

[0087] FIG. **5** shows a wireless energy transfer scheme featuring two capacitively loaded conducting-wire coils, and illustrates the surrounding field.

[0088] FIG. **6** shows an example of a resonant dielectric disk, and illustrates the surrounding field.

[0089] FIG. **7** shows a wireless energy transfer scheme featuring two resonant dielectric disks, and illustrates the surrounding field.

[0090] FIGS. **8***a* and **8***b* show schematics for frequency control mechanisms.

[0091] FIGS. **9***a* through **9***c* illustrate a wireless energy transfer scheme in the presence of various extraneous objects.

[0092] FIG. **10** illustrates a circuit model for wireless energy transfer.

[0093] FIG. **11** illustrates the efficiency of a wireless energy transfer scheme.

[0094] FIG. **12** illustrates parametric dependences of a wireless energy transfer scheme.

[0095] FIG. **13** plots the parametric dependences of a wireless energy transfer scheme.

[0096] FIG. **14** is a schematic of an experimental system demonstrating wireless energy transfer.

[0097] FIGS. **15-17**. Plot experiment results for the system shown schematically in FIG. **14**.

DETAILED DESCRIPTION

[0098] FIG. **1** shows a schematic that generally describes one embodiment of the invention, in which energy is transferred wirelessly between two resonant objects.

[0099] Referring to FIG. **1**, energy is transferred, over a distance D, between a resonant source object having a characteristic size L_1 and a resonant device object of characteristic size L_2. Both objects are resonant objects. The source object is connected to a power supply (not shown), and the device object is connected to a power consuming device (e.g. a load resistor, not shown). Energy is provided by the power supply to the source object, transferred wirelessly and non-radiatively from the source object to the device object, and consumed by the power consuming device. The wireless non-radiative energy transfer is performed using the field (e.g. the electromagnetic field or acoustic field) of the system of two resonant objects. For simplicity, in the following we will assume that field is the electromagnetic field.

[0100] It is to be understood that while two resonant objects are shown in the embodiment of FIG. **1**, and in many of the examples below, other embodiments may feature 3 or more resonant objects. For example, in some embodiments a single source object can transfer energy to multiple device objects. In some embodiments energy may be transferred from a first device to a second, and then from the second device to the third, and so forth.

[0101] Initially, we present a theoretical framework for understanding non-radiative wireless energy transfer. Note however that it is to be understood that the scope of the invention is not bound by theory.

[0102] Coupled Mode Theory

[0103] An appropriate analytical framework for modeling the resonant energy-exchange between two resonant objects **1** and **2** is that of "coupled-mode theory" (CMT). The field of the system of two resonant objects **1** and **2** is approximated by $F(r,t)\approx a_1(t)F_1(r)+a_2(t)F_2(r)$, where $F_{1,2}(r)$ are the eigenmodes of **1** and **2** alone, normalized to unity energy, and the field amplitudes $a_{1,2}(t)$ are defined so that $|a_{1,2}(t)|^2$ is equal to the energy stored inside the objects **1** and **2** respectively. Then, the field amplitudes can be shown to satisfy, to lowest order:

$$\frac{da_1}{dt} = -i(\omega_1 - i\Gamma_1)a_1 + i\kappa a_2 \qquad (1)$$
$$\frac{da_2}{dt} = -i(\omega_2 - i\Gamma_2)a_2 + i\kappa a_1,$$

where $\omega_{1,2}$ are the individual angular eigenfrequencies of the eigenmodes, $\Gamma_{1,2}$ are the resonance widths due to the objects' intrinsic (absorption, radiation etc.) losses, and K is the coupling coefficient. Eqs. (1) show that at exact resonance ($\omega_1=\omega_2$ and $\Gamma_1=\Gamma_2$), the eigenmodes of the combined system are split by 2κ; the energy exchange between the two objects takes place in time $\sim\pi/2\kappa$ and is nearly perfect, apart for losses, which are minimal when the coupling rate is much faster than all loss rates ($\kappa \gg \Gamma_{1,2}$). The coupling to loss ratio $\kappa/\sqrt{\Gamma_1\Gamma_2}$ serves as a figure-of-merit in evaluating a system used for wireless energy-transfer, along with the distance over which this ratio can be achieved. The regime $\kappa/\sqrt{\Gamma_1\Gamma_2} \gg 1$ is called "strong-coupling" regime.

[0104] In some embodiments, the energy-transfer application preferably uses resonant modes of high $Q=\omega/2\Gamma$, corresponding to low (i.e. slow) intrinsic-loss rates Γ. This condition may be satisfied where the coupling is implemented using, not the lossy radiative far-field, but the evanescent (non-lossy) stationary near-field.

[0105] To implement an energy-transfer scheme, usually finite objects, namely ones that are topologically surrounded everywhere by air, are more appropriate. Unfortunately, objects of finite extent cannot support electromagnetic states that are exponentially decaying in all directions in air, since, from Maxwell's Equations in free space: $\vec{k}^2=\omega^2/c^2$ where $\vec{k}$ is the wave vector, ω the angular frequency, and c the speed of light. Because of this, one can show that they cannot support states of infinite Q. However, very long-lived (so-called "high-Q") states can be found, whose tails display the needed exponential or exponential-like decay away from the resonant object over long enough distances before they turn oscillatory (radiative). The limiting surface, where this change in the field behavior happens, is called the "radiation caustic", and, for the wireless energy-transfer scheme to be based on the near field rather than the far/radiation field, the distance between the coupled objects must be such that one lies within the radiation caustic of the other.

[0106] Furthermore, in some embodiments, small $Q_\kappa=\omega/2\kappa$ corresponding to strong (i.e. fast) coupling rate κ is preferred over distances larger than the characteristic sizes of the objects. Therefore, since the extent of the near-field into the area surrounding a finite-sized resonant object is set typically by the wavelength, in some embodiments, this mid-range non-radiative coupling can be achieved using resonant objects of subwavelength size, and thus significantly longer evanescent field-tails. As will be seen in examples later on, such subwavelength resonances can often be accompanied with a high Q, so this will typically be the appropriate choice for the possibly-mobile resonant device-object. Note, though, that in some embodiments, the resonant source-object will be immobile and thus less restricted in its allowed geometry and size, which can be therefore chosen large enough that the near-field extent is not limited by the wavelength. Objects of nearly infinite extent, such as dielectric waveguides, can support guided modes whose evanescent tails are decaying exponentially in the direction away from the object, slowly if tuned close to cutoff, and can have nearly infinite Q.

[0107] In the following, we describe several examples of systems suitable for energy transfer of the type described above. We will demonstrate how to compute the CMT parameters $\omega_{1,2}$, $Q_{1,2}$ and Q_κ described above and how to choose these parameters for particular embodiments in order to produce a desirable figure-of-merit $\kappa/\sqrt{\Gamma_1\Gamma_2}=\sqrt{Q_1Q_2}/Q_\kappa$. In particular, this figure of merit is typically maximized when $\omega_{1,2}$ are tuned to a particular angular frequency ω, thus, if Γ is half the angular-frequency width for which $\sqrt{Q_1Q_2}/Q_\kappa$ is above half its maximum value at ω, the angular eigenfrequencies $\omega_{1,2}$ should typically be tuned to be close to ω to within the width Γ.

[0108] In addition, as described below, $Q_{1,2}$ can sometimes be limited not from intrinsic loss mechanisms but from external perturbations. In those cases, producing a desirable figure-of-merit translates to reducing Q_κ (i.e. increasing the coupling). Accordingly we will demonstrate how, for particular embodiments, to reduce Q_κ.

[0109] Self-Resonant Conducting Coils

[0110] In some embodiments, one or more of the resonant objects are self-resonant conducting coils. Referring to FIG. **2**, a conducting wire of length l and cross-sectional radius a is wound into a helical coil of radius r and height h (namely with $N=\sqrt{l^2-h^2}/2\pi r$ number of turns), surrounded by air. As described below, the wire has distributed inductance and distributed capacitance, and therefore it supports a resonant mode of angular frequency ω. The nature of the resonance lies in the periodic exchange of energy from the electric field within the capacitance of the coil, due to the charge distribution ρ(x) across it, to the magnetic field in free space, due to the current distribution j(x) in the wire. In particular, the charge conservation equation $\nabla\cdot j=i\omega\rho$ implies that: (i) this periodic exchange is accompanied by a π/2 phase-shift between the current and the charge density profiles, namely the energy U contained in the coil is at certain points in time completely due to the current and at other points in time completely due to the charge, and (ii) if ρ_l (x) and I(x) are respectively the linear charge and current densities in the wire, where x runs along the wire,

$$q_o=\frac{1}{2}\int dx|\rho_l(x)|$$

is the maximum amount of positive charge accumulated in one side of the coil (where an equal amount of negative charge always also accumulates in the other side to make the system neutral) and $I_o=\max\{|I(x)|\}$ is the maximum positive value of the linear current distribution, then $I_o=\omega q_o$. Then, one can define an effective total inductance L and an effective total capacitance C of the coil through the amount of energy U inside its resonant mode:

$$U\equiv\frac{1}{2}I_o^2L\Rightarrow L=\frac{\mu_o}{4\pi I_o^2}\int\int dxdx'\frac{j(x)\cdot j(x')}{|x-x'|}, \tag{2}$$

$$U\equiv\frac{1}{2}q_o^2\frac{1}{C}\Rightarrow\frac{1}{C}=\frac{1}{4\pi\varepsilon_o q_o^2}\int\int dxdx'\frac{\rho(x)\cdot\rho(x')}{|x-x'|}, \tag{3}$$

where μ_o and $\in_o$ are the magnetic permeability and electric permittivity of free space. With these definitions, the resonant angular frequency and the effective impedance are given by the common formulas $\omega=1/\sqrt{LC}$ and $Z=\sqrt{L/C}$ respectively.

[0111] Losses in this resonant system consist of ohmic (material absorption) loss inside the wire and radiative loss into free space. One can again define a total absorption resistance R_{abs} from the amount of power absorbed inside the wire and a total radiation resistance R_{rad} from the amount of power radiated due to electric- and magnetic-dipole radiation:

$$P_{abs}\equiv\frac{1}{2}I_o^2R_{abs}\Rightarrow R_{abs}\approx\zeta_c\frac{l}{2\pi a}\cdot\frac{I_{rms}^2}{I_o^2} \tag{4}$$

$$P_{rad}\equiv\frac{1}{2}I_o^2R_{rad}\Rightarrow R_{rad}\approx\frac{\zeta_o}{6\pi}\left[\left(\frac{\omega|p|}{c}\right)^2+\left(\frac{\omega\sqrt{|m|}}{c}\right)^4\right], \tag{5}$$

where $c=1/\sqrt{\mu_o\in_o}$ and $\zeta_o=\sqrt{\mu_o/\in_o}$ are the light velocity and light impedance in free space, the impedance ζ_c is $\zeta_c=1/\sigma\zeta=\sqrt{\mu_o\omega/2\sigma}$ with σ the conductivity of the conductor and δ the skin depth at the frequency ω,

$$I_{rms}^2=\frac{1}{l}\int dx|I(x)|^2,$$

$p=\int dx\, r\sigma_l(x)$ is the electric-dipole moment of the coil and

$$m=\frac{1}{2}\int dx r\times j(x)$$

is the magnetic-dipole moment of the coil. For the radiation resistance formula Eq. (5), the assumption of operation in the quasi-static regime ($h, r\ll\lambda=2\pi c/\omega$) has been used, which is the desired regime of a subwavelength resonance. With these definitions, the absorption and radiation quality factors of the resonance are given by $Q^{abs}=Z/R_{abs}$ and $Q^{rad}=Z/R_{rad}$ respectively.

[0112] From Eq. (2)-(5) it follows that to determine the resonance parameters one simply needs to know the current distribution j in the resonant coil. Solving Maxwell's equations to rigorously find the current distribution of the resonant electromagnetic eigenmode of a conducting-wire coil is more involved than, for example, of a standard LC circuit, and we can find no exact solutions in the literature for coils of finite length, making an exact solution difficult. One could in principle write down an elaborate transmission-line-like model, and solve it by brute force. We instead present a model that is (as described below) in good agreement (~5%) with experiment. Observing that the finite extent of the conductor forming each coil imposes the boundary condition that the current has to be zero at the ends of the coil, since no current can leave the wire, we assume that the resonant mode of each coil is well approximated by a sinusoidal current profile along the length of the conducting wire. We shall be interested in the lowest mode, so if we denote by x the coordinate along the conductor, such that it runs from −l/2 to +l/2, then the current amplitude profile would have the form $I(x)=I_o\cos(\zeta x/l)$, where we have assumed that the current does not vary significantly along the wire circumference for a particular x, a valid assumption provided $a\ll r$. It immediately follows from the continuity equation for charge that the linear charge density profile should be of the form $\rho_l(x)=\rho_o\sin(\pi x/l)$, and thus $q_o=\int_0^{l/2}dx\rho_o|\sin(\pi x/l)|=\rho_o l/\pi$. Using these sinusoidal profiles we find the so-called "self-inductance" L_s and "self-capacitance" C_s, of the coil by computing numerically the integrals Eq. (2) and (3); the associated frequency and effective impedance are ω_s and Z_s respectively. The "self-resistances" R_s are given analytically by Eq. (4) and (5) using

$$I_{rms}^2=\frac{1}{l}\int_{-l/2}^{l/2}dx|I_o\cos(\pi x/l)|^2=\frac{1}{2}I_o^2,$$

$$|p|=q_o\sqrt{\left(\frac{2}{h}h\right)^2+\left(\frac{4N\cos(\pi N)}{(4N^2-1)\pi}r\right)^2}$$

and

$$|m| = I_o\sqrt{\left(\frac{2}{\pi}N\pi r^2\right)^2 + \left(\frac{\cos(\pi N)(12N^2-1) - \sin(\pi N)\pi N(4N^2-1)}{(16N^4-8N^2+1)\pi}hr\right)^2},$$

and therefore the associated Q_s, factors may be calculated.

[0113] The results for two particular embodiments of resonant coils with subwavelength modes of $\lambda_s/r \geqq 70$ (i.e. those highly suitable for near-field coupling and well within the quasi-static limit) are presented in Table 1. Numerical results are shown for the wavelength and absorption, radiation and total loss rates, for the two different cases of subwavelength-coil resonant modes. Note that, for conducting material, copper (σ=5.998·10^−7 S/m) was used. It can be seen that expected quality factors at microwave frequencies are $Q_s^{abs} \geqq 1000$ and $Q_s^{rad} \geqq 5000$.

TABLE 1

single coil	λ_s/r	f(MHz)	Q_s^{rad}	Q_s^{abs}	$Q_s = \omega_s/2\Gamma_s$
r = 30 cm, h = 20 cm, a = 1 cm, N = 4	74.7	13.39	4164	8170	2758
r = 10 cm, h = 3 cm, a = 2 mm, N = 6	140	21.38	43919	3968	3639

[0114] Referring to FIG. **3**, in some embodiments, energy is transferred between two self-resonant conducting-wire coils. The electric and magnetic fields are used to couple the different resonant conducting-wire coils at a distance D between their centers. Usually, the electric coupling highly dominates over the magnetic coupling in the system under consideration for coils with h≫2r and, oppositely, the magnetic coupling highly dominates over the electric coupling for coils with h ≪2r. Defining the charge and current distributions of two coils **1**,**2** respectively as $\rho_{1,2}(x)$ and $j_{1,2}(x)$, total charges and peak currents respectively as $q_{1,2}$ and $I_{1,2}$, and capacitances and inductances respectively as $C_{1,2}$ and $L_{1,2}$, which are the analogs of $\rho(x)$, $j(x)$, q_o, I_o, C and L for the single-coil case and are therefore well defined, we can define their mutual capacitance and inductance through the total energy:

$$U \equiv U_1 + U_2 + \frac{1}{2}(q_1^* q_2 + q_2^* q_1)/M_C + \frac{1}{2}(I_1^* I_2 + I_2^* I_1)M_L \quad (6)$$

$$\Rightarrow 1/M_C = \frac{1}{4\pi\varepsilon_o q_1 q_2}\int\int dx dx' \frac{\rho_1(x)\cdot\rho_2(x')}{|x-x'|}u,$$

$$M_L = \frac{\mu_o}{4\pi I_1 I_2}\int\int dx dx' \frac{j_1(x)\cdot j_2(x')}{|x-x'|}u,$$

where

$$U_1 = \frac{1}{2}q_1^2/C_1 = \frac{1}{2}I_1^2 L_1,\ U_2 = \frac{1}{2}q_2^2/C_2 = \frac{1}{2}I_2^2 L_2$$

and the retardation factor of $u=\exp(i\omega|x-x'/c)$ inside the integral can been ignored in the quasi-static regime D≪λof interest, where each coil is within the near field of the other. With this definition, the coupling coefficient is given by $\kappa=\omega\sqrt{C_1C_2}/2M_C+\omega M_L/2\sqrt{L_1L_2} \Leftrightarrow Q_\kappa^{-1}=(M_C/\sqrt{C_1C_2})^{-1}+(\sqrt{L_1L_2}/M_L)^{-1}$.

[0115] Therefore, to calculate the coupling rate between two self-resonant coils, again the current profiles are needed and, by using again the assumed sinusoidal current profiles, we compute numerically from Eq. (6) the mutual capacitance $M_{C,s}$ and inductance $M_{L,s}$ between two self-resonant coils at a distance D between their centers, and thus $Q_{\kappa,s}$ is also determined

TABLE 2

pair of coils	D/r	Q = ω/2Γ	Q_κ = ω/2κ	κ/Γ
r = 30 cm, h = 20 cm,	3	2758	38.9	70.9
a = 1 cm, N = 4	5	2758	139.4	19.8
λ/r ≈ 75	7	2758	333.0	8.3
$Q_s^{abs} \approx 8170$, $Q_s^{rad} \approx 4164$	10	2758	818.9	3.4
r = 10 cm, h = 3 cm,	3	3639	61.4	59.3
a = 2 mm, N = 6	5	3639	232.5	15.7
λ/r ≈ 140	7	3639	587.5	6.2

TABLE 2-continued

pair of coils	D/r	Q = ω/2Γ	Q_κ = ω/2κ	κ/Γ
$Q_s^{abs} \approx 3968$, $Q_s^{rad} \approx 43919$	10	3639	1580	2.3

[0116] Referring to Table 2, relevant parameters are shown for exemplary embodiments featuring pairs or identical self resonant coils. Numerical results are presented for the average wavelength and loss rates of the two normal modes (individual values not shown), and also the coupling rate and figure-of-merit as a function of the coupling distance D, for the two cases of modes presented in Table 1. It can be seen that for medium distances D/r=10−3 the expected coupling-to-loss ratios are in the range κ/Γ~2−70.

[0117] Capacitively-Loaded Conducting Loops or Coils

[0118] In some embodiments, one or more of the resonant objects are capacitively-loaded conducting loops or coils. Referring to FIG. **4** a helical coil with N turns of conducting wire, as described above, is connected to a pair of conducting parallel plates of area A spaced by distance d via a dielectric material of relative permittivity c, and everything is surrounded by air (as shown, N=1 and h=0). The plates have a capacitance $C_p=\in_o\in A/d$, which is added to the distributed capacitance of the coil and thus modifies its resonance. Note however, that the presence of the loading capacitor modifies significantly the current distribution inside the wire and therefore the total effective inductance L and total effective capacitance C of the coil are different respectively from L_s and C_s, which are calculated for a self-resonant coil of the same geometry using a sinusoidal current profile. Since some charge is accumulated at the plates of the external loading capacitor, the charge distribution ρ inside the wire is reduced, so $C<C_s$, and thus, from the charge conservation equation, the current distribution j flattens out, so $L>L_s$.

[0119] The resonant frequency for this system is $\omega=1/\sqrt{L(C+C_p)}<\omega_s=1\sqrt{L_sC_s}$, and $I(x)\rightarrow I_o \cos(\pi x/l)\Rightarrow C\rightarrow C_s \Rightarrow\omega\rightarrow\omega_s$, as $C_p\rightarrow 0$.

[0120] In general, the desired CMT parameters can be found for this system, but again a very complicated solution of Maxwell's Equations is required. Instead, we will analyze only a special case, where a reasonable guess for the current distribution can be made. When $C_p\gg C_s>C$, then $\omega\approx 1/\sqrt{LC_p} \ll\omega_s$ and $Z\approx\sqrt{L/C_p}\ll Z_s$, while all the charge is on the plates of the loading capacitor and thus the current distribution is constant along the wire. This allows us now to compute numerically L from Eq. (2). In the case h=0 and N integer, the integral in Eq. (2) can actually be computed analytically, giving the formula $L=\mu_o r\,[\ln(8r/a)-2]N^2$. Explicit analytical formulas are again available for R from Eq. (4) and (5), since $I_{rms}=I_o$, $|p|\approx 0$ and $|m|=I_oN\pi r^2$ (namely only the magnetic-dipole term is contributing to radiation), so we can determine also $Q^{abs}=\omega L/R_{abs}$ and $Q^{rad}=\omega L/R_{rad}$. At the end of the calculations, the validity of the assumption of constant current profile is confirmed by checking that indeed the condition $C_p \gg C_s\Leftrightarrow\omega\ll\omega_s$ is satisfied. To satisfy this condition, one could use a large external capacitance, however, this would usually shift the operational frequency lower than the optimal frequency, which we will determine shortly; instead, in typical embodiments, one often prefers coils with very small self-capacitance C_s to begin with, which usually holds, for the types of coils under consideration, when N=1, so that the self-capacitance comes from the charge distribution across the single turn, which is almost always very small, or when N>1 and $h\gg 2Na$, so that the dominant self-capacitance comes from the charge distribution across adjacent turns, which is small if the separation between adjacent turns is large.

[0121] The external loading capacitance C_p provides the freedom to tune the resonant frequency (for example by tuning A or d). Then, for the particular simple case h=0, for which we have analytical formulas, the total $Q=\omega L/(R_{abs}+R_{rad})$ becomes highest at the optimal frequency

$$\tilde{\omega}=\left[\frac{c^4}{\pi}\sqrt{\frac{\varepsilon_o}{2\sigma}}\cdot\frac{1}{aNr^3}\right]^{2/7}, \tag{7}$$

reaching the value

$$\tilde{Q}=\frac{6}{7\pi}\left(2\pi^2\eta_o\frac{\sigma a^2N^2}{r}\right)^{3/7}\cdot\left[\ln\left(\frac{8r}{a}\right)-2\right]. \tag{8}$$

[0122] At lower frequencies it is dominated by ohmic loss and at higher frequencies by radiation. Note, however, that the formulas above are accurate as long as $\omega\ll\omega_s$ and, as explained above, this holds almost always when N=1, and is usually less accurate when N>1, since h=0 usually implies a large self-capacitance. A coil with large h can be used, if the self-capacitance needs to be reduced compared to the external capacitance, but then the formulas for L and ω, Q are again less accurate. Similar qualitative behavior is expected, but a more complicated theoretical model is needed for making quantitative predictions in that case.

[0123] The results of the above analysis for two embodiments of subwavelength modes of $\lambda/r\geqq 70$ (namely highly suitable for near-field coupling and well within the quasi-static limit) of coils with N=1 and h=0 at the optimal frequency Eq. (7) are presented in Table 3. To confirm the validity of constant-current assumption and the resulting analytical formulas, mode-solving calculations were also performed using another completely independent method: computational 3D finite-element frequency-domain (FEFD) simulations (which solve Maxwell's Equations in frequency domain exactly apart for spatial discretization) were conducted, in which the boundaries of the conductor were modeled using a complex impedance $\zeta_c=\sqrt{\mu_o\omega/2\sigma}$ boundary condition, valid as long as $\zeta_c/\zeta_o\ll 1$ ($<10^{-5}$ for copper in the microwave). Table 3 shows Numerical FEFD (and in parentheses analytical) results for the wavelength and absorption, radiation and total loss rates, for two different cases of subwavelength-loop resonant modes. Note that for conducting material copper ($\sigma=5.998\cdot 10^7$ S/m) was used. (The specific parameters of the plot in FIG. **4** are highlighted with bold in the table.) The two methods (analytical and computational) are in very good agreement and show that, in some embodiments, the optimal frequency is in the low-MHz microwave range and the expected quality factors are $Q^{abs}\geqq 1000$ and $Q^{rad}\geqq 10000$.

TABLE 3

single coil	λ/r	f(MHz)	Q^{rad}	Q^{abs}	$Q=\omega/2\Gamma$
r = 30 cm, a = 2 cm	**111.4 (112.4)**	**8.976 (8.897)**	**29546 (30512)**	**4886 (5117)**	**4193 (4381)**
ϵ = 10, A = 138 cm^2, d = 4 mm					
r = 10 cm, a = 2 mm	69.7 (70.4)	43.04 (42.61)	10702 (10727)	1545 (1604)	1350 (1395)
ϵ = 10, A = 3.14 cm^2, d = 1 mm					

[0124] Referring to FIG. **5**, in some embodiments, energy is transferred between two capacitively-loaded coils **1** and **2** at distance D between their centers, the mutual inductance M_L can be evaluated numerically from Eq. (6) by using constant current distributions in the case $\omega\ll\omega_s$. In the case h=0, the coupling is only magnetic and again we have an analytical formula, which, in the quasi-static limit $r\ll D\ll\lambda$ and for the relative orientation shown in FIG. **4**, is $M_L\approx\pi\mu_o/2\cdot(r_1r_2)^2N_1N_2/D^3$, which means that $Q_\kappa\propto(D/\sqrt{r_1r_2})^3$ is independent of the frequency ω and the number of turns N_1, N_2. Consequently, the resultant coupling figure-of-merit of interest is

$$\frac{\kappa}{\sqrt{\Gamma_1\Gamma_2}}=\frac{\sqrt{Q_1Q_2}}{Q_\kappa}\approx\left(\frac{\sqrt{r_1r_2}}{D}\right)^3\cdot\frac{\pi^2\eta_o\frac{\sqrt{r_1r_2}}{\lambda}\cdot N_1N_2}{\prod_{j=1,2}\left(\sqrt{\frac{\pi\eta_o}{\lambda\sigma}}\cdot\frac{r_j}{a_j}N_j+\frac{8}{3}\pi^5\eta_o\left(\frac{r_j}{\lambda}\right)^4N_j^2\right)^{1/2}}, \tag{9}$$

which again is more accurate for $N_1=N_2=1$.

[0125] From Eq. (9) it can be seen that the optimal frequency ω, where the figure-of-merit is maximized to the value $\sqrt{Q_1Q_2}/Q_\kappa$), is that where $\sqrt{Q_1Q_2}$ is maximized, since Q_κ does not depend on frequency (at least for the distances $D<<\lambda$ of interest for which the quasi-static approximation is still valid). Therefore, the optimal frequency is independent of the distance D between the two coils and lies between the two frequencies where the single-coil Q_1 and Q_2 peak. For same coils, it is given by Eq. (7) and then the figure-of-merit Eq. (9) becomes

$$\left(\frac{\tilde{\kappa}}{\Gamma}\right)=\frac{\tilde{Q}}{Q_\kappa}\approx\left(\frac{r}{D}\right)^3\cdot\frac{3}{7}\left(2\pi^2\eta_o\frac{\sigma a^2N^2}{r}\right)^{3/7}. \quad (10)$$

Typically, one should tune the capacitively-loaded conducting loops or coils, so that their angular eigenfrequencies are close to ω within Γ, which is half the angular frequency width for which $\sqrt{Q_1Q_2}/Q_\kappa>\sqrt{Q_1Q_2}/Q_\kappa)/2$.

[0126] Referring to Table 4, numerical FEFD and, in parentheses, analytical results based on the above are shown for two systems each composed of a matched pair of the loaded coils described in Table 3. The average wavelength and loss rates are shown along with the coupling rate and coupling to loss ratio figure-of-merit κ/Γ as a function of the coupling distance D, for the two cases. Note that the average numerical Γ^{rad} shown are again slightly different from the single-loop value of FIG. **3**, analytical results for Γ^{rad} are not shown but the single-loop value is used. (The specific parameters corresponding to the plot in FIG. **5** are highlighted with bold in the table.) Again we chose N=1 to make the constant-current assumption a good one and computed M_L numerically from Eq. (6). Indeed the accuracy can be confirmed by their agreement with the computational FEFD mode-solver simulations, which give i through the frequency splitting (=2κ) of the two normal modes of the combined system. The results show that for medium distances D/r=10–3 the expected coupling-to-loss ratios are in the range κ/Γ~0.5–50.

TABLE 4

pair of coils	D/r	Q^{rad}	$Q=\omega/2\Gamma$	$Q_\kappa=\omega/2\kappa$	κ/Γ
r = 30 cm, a = 2 cm	3	30729	4216	62.6 (63.7)	67.4 (68.7)
ϵ = 10, A = 138 cm^2, d = 4 mm	5	29577	4194	235 (248)	17.8 (17.6)
$\lambda/r\approx 112$	**7**	**29128**	**4185**	**589 (646)**	**7.1 (6.8)**
$Q^{abs}\approx 4886$	10	28833	4177	1539 (1828)	2.7 (2.4)
r = 10 cm, a = 2 mm	3	10955	1355	85.4 (91.3)	15.9 (15.3)
ϵ = 10, A = 3.14 cm^2, d = 1 mm	5	10740	1351	313 (356)	4.32 (3.92)
$\lambda/r\approx 70$	7	10759	1351	754 (925)	1.79 (1.51)
$Q^{abs}\approx 1546$	10	10756	1351	1895 (2617)	0.71 (0.53)

[0127] Optimization of $\sqrt{Q_1Q_2}/Q_\kappa$

[0128] In some embodiments, the results above can be used to increase or optimize the performance of a wireless energy transfer system which employs capacitively-loaded coils. For example, the scaling of Eq. (10) with the different system parameters one sees that to maximize the system figure-of-merit κ/Γ one can, for example:

[0129] Decrease the resistivity of the conducting material. This can be achieved, for example, by using good conductors (such as copper or silver) and/or lowering the temperature. At very low temperatures one could use also superconducting materials to achieve extremely good performance.

[0130] Increase the wire radius a. In typical embodiments, this action is limited by physical size considerations. The purpose of this action is mainly to reduce the resistive losses in the wire by increasing the cross-sectional area through which the electric current is flowing, so one could alternatively use also a Litz wire or a ribbon instead of a circular wire.

[0131] For fixed desired distance D of energy transfer, increase the radius of the loop r. In typical embodiments, this action is limited by physical size considerations.

[0132] For fixed desired distance vs. loop-size ratio D/r, decrease the radius of the loop r. In typical embodiments, this action is limited by physical size considerations.

[0133] Increase the number of turns N. (Even though Eq. (10) is expected to be less accurate for N>1, qualitatively it still provides a good indication that we expect an improvement in the coupling-to-loss ratio with increased N.) In typical embodiments, this action is limited by physical size and possible voltage considerations, as will be discussed in following sections.

[0134] Adjust the alignment and orientation between the two coils. The figure-of-merit is optimized when both cylindrical coils have exactly the same axis of cylindrical symmetry (namely they are "facing" each other). In some embodiments, particular mutual coil angles and orientations that lead to zero mutual inductance (such as the orientation where the axes of the two coils are perpendicular) should be avoided.

[0135] Finally, note that the height of the coil h is another available design parameter, which has an impact to the performance similar to that of its radius r, and thus the design rules are similar.

[0136] The above analysis technique can be used to design systems with desired parameters. For example, as listed below, the above described techniques can be used to determine the cross sectional radius a of the wire which one should use when designing as system two same single-turn loops with a given radius in order to achieve a specific performance in terms of κ/Γ at a given D/r between them, when the material is copper ($\sigma=5.998\cdot10^7$S/m):

[0137] D/r=5, $\kappa/\Gamma\geqq10$, r=30 cm$\Rightarrow$a$\geqq$9 mm

[0138] D/r=5, $\kappa/\Gamma\geqq10$, r=5 cm$\Rightarrow$a$\geqq$3.7 mm

[0139] D/r=5, $\kappa/\Gamma\geqq20$, r=30 cm$\Rightarrow$a$\geqq$20 mm

[0140] D/r=5, $\kappa/\Gamma\geqq20$, r=5 cm$\Rightarrow$a$\geqq$8.3 mm

[0141] D/r=10, $\kappa/\Gamma\geqq1$, r=30 cm$\Rightarrow$a$\geqq$7 mm

[0142] D/r=10, $\kappa/\Gamma\geqq1$, r=5 cm$\Rightarrow$a$\geqq$2.8 mm

[0143] D/r=10, $\kappa/\Gamma\geqq3$, r=30 cm$\Rightarrow$a$\geqq$25 mm

[0144] D/r=10, $\kappa/\Gamma\geqq3$, r=5 cm$\Rightarrow$a$\geqq$10 mm

[0145] Similar analysis can be done for the case of two dissimilar loops. For example, in some embodiments, the device under consideration is very specific (e.g. a laptop or a cell phone), so the dimensions of the device object (r_d, h_d, a_d, N_d) are very restricted. However, in some such embodiments, the restrictions on the source object (r_s, h_s, a_s, N_s) are much less, since the source can, for example, be placed under the floor or on the ceiling. In such cases, the desired distance is often well defined, based on the application (e.g. D~1 m for charging a laptop on a table wirelessly from the floor). Listed below are examples (simplified to the case $N_s=N_d=1$ and $h_s=h_d=0$) of how one can vary the dimensions of the source object to achieve the desired system performance in terms of $\kappa/\sqrt{\Gamma_s\Gamma_d}$, when the material is again copper ($\sigma=5.998\cdot10^7$ S/m):

$D = 1.5$ m,

$\kappa/\sqrt{\Gamma_s\Gamma_d} \geq 15$,

$r_d = 30$ cm, $a_d = 6$ mm $\Rightarrow r_s = 1.158$ m,

$a_s \geq 5$ mm

$D = 1.5$, $\kappa/\sqrt{\Gamma_s\Gamma_d} \geq 30$,

$r_d = 30$ cm,

$a_d = 6$ mm $\Rightarrow r_s = 1.15$ m,

$a_s \geq 33$ mm

$D = 1.5$ m,

$\kappa/\sqrt{\Gamma_s\Gamma_d} \geq 1$,

$r_d = 5$ cm,

$a_d = 4$ mm $\Rightarrow r_s = 1.119$ m,

$a_s \geq 7$ mm

$D = 1.5$ m,

$\kappa/\sqrt{\Gamma_s\Gamma_d} \geq 2$,

$r_d = 5$ cm,

$a_d = 4$ mm $\Rightarrow r_s = 1.119$ m,

$a_s \geq 52$ mm

$D = 2$ m,

$\kappa/\sqrt{\Gamma_s\Gamma_d} \geq 10$,

$r_d = 30$ cm,

$a_d = 6$ mm $\Rightarrow r_s = 1.518$ m,

$a_s \geq 7$ mm

$D = 2$ m,

$\kappa/\sqrt{\Gamma_s\Gamma_d} \geq 20$,

$r_d = 30$ cm,

$a_d = 6$ mm $\Rightarrow r_s = 1.514$ m,

$a_s \geq 50$ mm

$D = 2$ m,

$\kappa/\sqrt{\Gamma_s\Gamma_d} \geq 0.5$,

$r_d = 5$ cm,

-continued

$a_d = 4$ mm $\Rightarrow r_s = 1.491$ m,

$a_s \geq 5$ mm

$D = 2$ m,

$\kappa/\sqrt{\Gamma_s\Gamma_d} \geq 1$,

$r_d = 5$ cm,

$a_d = 4$ mm $\Rightarrow r_s = 1.491$ m,

$a_s \geq 36$ mm

[0146] Optimization of Q_κ

[0147] As will be described below, in some embodiments the quality factor Q of the resonant objects is limited from external perturbations and thus varying the coil parameters cannot lead to improvement in Q. In such cases, one may opt to increase the coupling to loss ratio figure-of-merit by decreasing Q_κ (i.e. increasing the coupling). The coupling does not depend on the frequency and the number of turns. Therefore, the remaining degrees of freedom are:

[0148] Increase the wire radii a_1 and a_2. In typical embodiments, this action is limited by physical size considerations.

[0149] For fixed desired distance D of energy transfer, increase the radii of the coils r_1 and r_2. In typical embodiments, this action is limited by physical size considerations.

[0150] For fixed desired distance vs. coil-sizes ratio $D/\sqrt{r_1r_2}$, only the weak (logarithmic) dependence of the inductance remains, which suggests that one should decrease the radii of the coils r_1 and r_2. In typical embodiments, this action is limited by physical size considerations.

[0151] Adjust the alignment and orientation between the two coils. In typical embodiments, the coupling is optimized when both cylindrical coils have exactly the same axis of cylindrical symmetry (namely they are "facing" each other). Particular mutual coil angles and orientations that lead to zero mutual inductance (such as the orientation where the axes of the two coils are perpendicular) should obviously be avoided.

[0152] Finally, note that the heights of the coils h_1 and h_2 are other available design parameters, which have an impact to the coupling similar to that of their radii r_1 and r_2, and thus the design rules are similar.

[0153] Further practical considerations apart from efficiency, e.g. physical size limitations, will be discussed in detail below.

[0154] It is also important to appreciate the difference between the above described resonant-coupling inductive scheme and the well-known non-resonant inductive scheme for energy transfer. Using CMT it is easy to show that, keeping the geometry and the energy stored at the source fixed, the resonant inductive mechanism allows for ~Q^2 (~10^6) times more power delivered for work at the device than the traditional non-resonant mechanism. This is why only close-range contact-less medium-power (~W) transfer is possible with the latter, while with resonance either close-range but large-power (~kW) transfer is allowed or, as currently proposed, if one also ensures operation in the strongly-coupled regime, medium-range and medium-power transfer is possible.

Capacitively-loaded conducting loops are currently used as resonant antennas (for example in cell phones), but those operate in the far-field regime with $D/r \gg 1$, $r/\lambda \sim 1$, and the radiation Q's are intentionally designed to be small to make the antenna efficient, so they are not appropriate for energy transfer.

[0155] Inductively-Loaded Conducting Rods

[0156] A straight conducting rod of length 2h and cross-sectional radius a has distributed capacitance and distributed inductance, and therefore it supports a resonant mode of angular frequency ω. Using the same procedure as in the case of self-resonant coils, one can define an effective total inductance L and an effective total capacitance C of the rod through formulas (2) and (3). With these definitions, the resonant angular frequency and the effective impedance are given again by the common formulas $\omega=1/\sqrt{LC}$ and $Z=\sqrt{L/C}$ respectively. To calculate the total inductance and capacitance, one can assume again a sinusoidal current profile along the length of the conducting wire. When interested in the lowest mode, if we denote by x the coordinate along the conductor, such that it runs from −h to +h, then the current amplitude profile would have the form $I(x)=I_0 \cos(\pi x/2h)$, since it has to be zero at the open ends of the rod. This is the well-known half-wavelength electric dipole resonant mode.

[0157] In some embodiments, one or more of the resonant objects are inductively-loaded conducting rods. A straight conducting rod of length 2h and cross-sectional radius a, as in the previous paragraph, is cut into two equal pieces of length h, which are connected via a coil wrapped around a magnetic material of relative permeability μ, and everything is surrounded by air. The coil has an inductance L_c, which is added to the distributed inductance of the rod and thus modifies its resonance. Note however, that the presence of the center-loading inductor modifies significantly the current distribution inside the wire and therefore the total effective inductance L and total effective capacitance C of the rod are different respectively from L_s and C_s, which are calculated for a self-resonant rod of the same total length using a sinusoidal current profile, as in the previous paragraph. Since some current is running inside the coil of the external loading inductor, the current distribution j inside the rod is reduced, so $L<L_s$, and thus, from the charge conservation equation, the linear charge distribution σ_l flattens out towards the center (being positive in one side of the rod and negative in the other side of the rod, changing abruptly through the inductor), so $C>C_s$. The resonant frequency for this system is $\omega=1/\sqrt{(L+L_c)C}<\omega_s=\sqrt{L_sC_s}$, and $I(x)\rightarrow\cos(\pi x/2h) \Rightarrow L\rightarrow L_s \Rightarrow\omega\rightarrow\omega_s$, as $L_c\rightarrow 0$.

[0158] In general, the desired CMT parameters can be found for this system, but again a very complicated solution of Maxwell's Equations is required. Instead, we will analyze only a special case, where a reasonable guess for the current distribution can be made. When $L_c \gg L_s > L$, then $\omega\approx 1/\sqrt{L_cC} \ll \omega_s$ and $Z\approx\sqrt{L_c/C} \gg Z_S$, while the current distribution is triangular along the rod (with maximum at the center-loading inductor and zero at the ends) and thus the charge distribution is positive constant on one half of the rod and equally negative constant on the other side of the rod. This allows us now to compute numerically C from Eq. (3). In this case, the integral in Eq. (3) can actually be computed analytically, giving the formula $1/C=1/(\pi\in_o h)[\ln(h/a)-1]$. Explicit analytical formulas are again available for R from Eq. (4) and (5), since $I_{rms}=I_o$, $|p|=q_o h$ and $|m|=0$ (namely only the electric-dipole term is contributing to radiation), so we can determine also $Q^{abs}=1/\omega CR_{abs}$ and $Q^{rad}=1/\omega CR_{rad}$. At the end of the calculations, the validity of the assumption of triangular current profile is confirmed by checking that indeed the condition $L_c \gg L_s \Leftrightarrow \omega \ll_s$ is satisfied. This condition is relatively easily satisfied, since typically a conducting rod has very small self-inductance L_s to begin with.

[0159] Another important loss factor in this case is the resistive loss inside the coil of the external loading inductor L_c and it depends on the particular design of the inductor. In some embodiments, the inductor is made of a Brooks coil, which is the coil geometry which, for fixed wire length, demonstrates the highest inductance and thus quality factor. The Brooks coil geometry has N_{Bc} turns of conducting wire of cross-sectional radius a_{Bc} wrapped around a cylindrically symmetric coil former, which forms a coil with a square cross-section of side r_{Bc}, where the inner side of the square is also at radius r_{Bc} (and thus the outer side of the square is at radius $2r_{Bc}$), therefore $N_{Bc}\approx(r_{Bc}/2a_{Bc})$. The inductance of the coil is then $L_c=2.0285\mu_o r_{Bc} N_{Bc}^2\approx 2.0285\mu_o r_{Bc}^5/8a_{Bc}^4$ and its resistance

$$R_C \approx \frac{1}{\sigma}\frac{l_{Bc}}{\pi a_{Bc}^2}\sqrt{1+\frac{\mu_o\omega\sigma}{2}\left(\frac{a_{Bc}}{2}\right)^2},$$

where the total wire length is $l_{Bc}\approx 2\pi(3r_{Bc}/2)N_{Bc}\approx 3\pi r_{Bc}^3/4a_{Bc}^2$ and we have used an approximate square-root law for the transition of the resistance from the dc to the ac limit as the skin depth varies with frequency.

[0160] The external loading inductance L_c provides the freedom to tune the resonant frequency. (For example, for a Brooks coil with a fixed size r_{Bc}, the resonant frequency can be reduced by increasing the number of turns N_{Bc} by decreasing the wire cross-sectional radius a_{Bc}. Then the desired resonant angular frequency $\omega=1/\sqrt{L_cC}$ is achieved for $a_{Bc}\approx(2.0285\mu_o r_{Bc}^5\omega^2 C)^{1/4}$ and the resulting coil quality factor is

$$Q_c \approx 0.169\mu_o\sigma r_{Bc}^2\omega \Big/ \sqrt{1+\omega^2\mu_o\sigma\sqrt{2.0285\mu_o(r_{Bc}/4)^5 C}}\,.$$

Then, for the particular simple case $L_c \gg L_s$, for which we have analytical formulas, the total $Q=1\omega C(R_c+R_{abs}+R_{rad})$ becomes highest at some optimal frequency ϖ, reaching the value Ϙ, both determined by the loading-inductor specific design. (For example, for the Brooks-coil procedure described above, at the optimal frequency $\varpi\approx Q_c\approx 0.8(\mu_o\sigma^2 r_{Bc}^3/C)^{1/4}$) At lower frequencies it is dominated by ohmic loss inside the inductor coil and at higher frequencies by radiation. Note, again, that the above formulas are accurate as long as $\varpi \ll \omega_s$ and, as explained above, this is easy to design for by using a large inductance.

[0161] The results of the above analysis for two embodiments, using Brooks coils, of subwavelength modes of $\lambda/h \geqq 200$ (namely highly suitable for near-field coupling and well within the quasi-static limit) at the optimal frequency ϖ are presented in Table 5. Table 5 shows in parentheses (for similarity to previous tables) analytical results for the wavelength and absorption, radiation and total loss rates, for two different cases of subwavelength-loop resonant modes. Note that for conducting material copper ($\sigma=5.998\cdot 10^7$ S/m) was used. The results show that, in some embodiments, the optimal frequency is in the low-MHz microwave range and the expected quality factors are $Q^{abs}\geqq 1000$ and $Q^{rad}\geqq 100000$.

TABLE 5

single rod	λ/h	f(MHz)	Q^{rad}	Q^{abs}	$Q = \omega/2\Gamma$
h = 30 cm, a = 2 cm μ = 1, r_{Bc} = 2 cm, a_{Bc} = 0.88 mm, N_{Bc} = 129	(403.8)	(2.477)	(2.72 * 10^6)	(7400)	(7380)
h = 10 cm, a = 2 mm μ = 1, r_{Bc} = 5 mm, a_{Bc} = 0.25 mm,	(214.2)	(14.010)	(6.92 * 10^5)	(3908)	(3886)

[0162] In some embodiments, energy is transferred between two inductively-loaded rods. For the rate of energy transfer between two inductively-loaded rods **1** and **2** at distance D between their centers, the mutual capacitance M_c can be evaluated numerically from Eq. (6) by using triangular current distributions in the case $\omega \ll \omega_s$. In this case, the coupling is only electric and again we have an analytical formula, which, in the quasi-static limit $h \ll D \ll \lambda$ and for the relative orientation such that the two rods are aligned on the same axis, is $1/M_c \approx 1/2\pi\in_o \cdot (h_1 h_2)^2/D^3$, which means that $Q_\kappa \propto (D/\sqrt{h_1 h_2})^3$ is independent of the frequency ω. Consequently, one can get the resultant coupling figure-of-merit of interest

$$\frac{\kappa}{\sqrt{\Gamma_1\Gamma_2}} = \frac{\sqrt{Q_1 Q_2}}{Q_\kappa}.$$

It can be seen that the optimal frequency ω, where the figure-of-merit is maximized to the value $\sqrt{Q_1Q_2}/Q_\kappa)$, is that where $\sqrt{Q_1Q_2}$ is maximized, since Q_κ, does not depend on frequency (at least for the distances $D \ll \lambda$ of interest for which the quasi-static approximation is still valid). Therefore, the optimal frequency is independent of the distance D between the two rods and lies between the two frequencies where the single-rod Q_1 and Q_2 peak. Typically, one should tune the inductively-loaded conducting rods, so that their angular eigenfrequencies are close to ω within Γ, which is half the angular frequency width for which $\sqrt{Q_1Q_2}/Q_\kappa > \sqrt{Q_1Q_2}/Q_\kappa)/2$.

[0163] Referring to Table 6, in parentheses (for similarity to previous tables) analytical results based on the above are shown for two systems each composed of a matched pair of the loaded rods described in Table 5. The average wavelength and loss rates are shown along with the coupling rate and coupling to loss ratio figure-of-merit κ/Γ as a function of the coupling distance D, for the two cases. Note that for Γ^{rad} the single-rod value is used. Again we chose $L_c \gg L_s$ to make the triangular-current assumption a good one and computed M_c numerically from Eq. (6). The results show that for medium distances D/h=10–3 the expected coupling-to-loss ratios are in the range κ/Γ~0.5–100.

TABLE 6

pair of rods	D/h	$Q_\kappa = \omega/2\kappa$	κ/Γ
h = 30 cm, a = 2 cm	3	(70.3)	(105.0)
μ = 1, r_{Bc} = 2 cm,	5	(389)	(19.0)
a_{Bc} = 0.88 mm, N_{Bc} = 129	7	(1115)	(6.62)
λ/h ≈ 404	10	(3321)	(2.22)
Q ≈ 7380			
h = 10 cm, a = 2 mm	3	(120)	(32.4)
μ = 1, r_{Bc} = 5 mm,	5	(664)	(5.85)

TABLE 6-continued

pair of rods	D/h	$Q_\kappa = \omega/2\kappa$	κ/Γ
a_{Bc} = 0.25 mm, N_{Bc} = 103	7	(1900)	(2.05)
λ/h ≈ 214	10	(5656)	(0.69)
Q ≈ 3886			

[0164] Dielectric Disks

[0165] In some embodiments, one or more of the resonant objects are dielectric objects, such as disks. Consider a two dimensional dielectric disk object, as shown in FIG. **6**, of radius r and relative permittivity c surrounded by air that supports high-Q "whispering-gallery" resonant modes. The loss mechanisms for the energy stored inside such a resonant system are radiation into free space and absorption inside the disk material. High-Q_{rad} and long-tailed subwavelength resonances can be achieved when the dielectric permittivity c is large and the azimuthal field variations are slow (namely of small principal number m). Material absorption is related to the material loss tangent: $Q_{abs} \sim \mathrm{Re}\{\in\}/\mathrm{Im}\{\in\}$. Mode-solving calculations for this type of disk resonances were performed using two independent methods: numerically, 2D finite-difference frequency-domain (FDFD) simulations (which solve Maxwell's Equations in frequency domain exactly apart for spatial discretization) were conducted with a resolution of 30 pts/r; analytically, standard separation of variables (SV) in polar coordinates was used.

TABLE 7

single disk	λ/r	Q^{abs}	Q^{rad}	Q
$\mathrm{Re}\{\epsilon\}$ = 47.7, m = 2	**20.01 (20.00)**	**10103 (10075)**	**1988 (1992)**	**1661 (1663)**
$\mathrm{Re}\{\epsilon\}$ = 65.6, m = 3	9.952 (9.950)	10098 (10087)	9078 (9168)	4780 (4802)

[0166] The results for two TE-polarized dielectric-disk subwavelength modes of $\lambda/r \geqq 10$ are presented in Table 7. Table 7 shows numerical FDFD (and in parentheses analytical SV) results for the wavelength and absorption, radiation and total loss rates, for two different cases of subwavelength-disk resonant modes. Note that disk-material loss-tangent $\mathrm{Im}\{\in\}/\mathrm{Re}\{\in\} = 10^{-4}$ was used. (The specific parameters corresponding to the plot in FIG. **6**. are highlighted with bold in the table.) The two methods have excellent agreement and imply that for a properly designed resonant low-loss-dielectric object values of $Q_{rad} \geqq 2000$ and $Q_{abs} \sim 10000$ are achievable. Note that for the 3D case the computational complexity would be immensely increased, while the physics would not

be significantly different. For example, a spherical object of $\in$=147.7 has a whispering gallery mode with m=2, Qrad=13962, and λ/r=17.

[0167] The required values of $\in$, shown in Table 7, might at first seem unrealistically large. However, not only are there in the microwave regime (appropriate for approximately meter-range coupling applications) many materials that have both reasonably high enough dielectric constants and low losses (e.g. Titania, Barium tetratitanate, Lithium tantalite etc.), but also c could signify instead the effective index of other known subwavelength surface-wave systems, such as surface modes on surfaces of metallic materials or plasmonic (metal-like, negative-$\in$) materials or metallo-dielectric photonic crystals or plasmono-dielectric photonic crystals.

[0168] To calculate now the achievable rate of energy transfer between two disks **1** and **2**, as shown in FIG. **7** we place them at distance D between their centers. Numerically, the FDFD mode-solver simulations give κ through the frequency splitting (=2κ) of the normal modes of the combined system, which are even and odd superpositions of the initial single-disk modes; analytically, using the expressions for the separation-of-variables eigenfields $E_{1,2}(r)$CMT gives κ through $\kappa=\omega_1/2\cdot\int d^3r\in_2(r)E_2^*(r)E_1(r)/\int d^3r\in(r)|E_1(r)|^2$ where $\in_j(r)$ and $\in(r)$ are the dielectric functions that describe only the disk j (minus the constant $\in_o$ background) and the whole space respectively. Then, for medium distances D/r=10–3 and for non-radiative coupling such that $D<2r_c$, where $r_c=m\lambda/2\zeta$ is the radius of the radiation caustic, the two methods agree very well, and we finally find, as shown in Table 8, coupling-to-loss ratios in the range κ/Γ~1-50. Thus, for the analyzed embodiments, the achieved figure-of-merit values are large enough to be useful for typical applications, as discussed below.

TABLE 8

two disks	D/r	Q^{rad}	Q = $\omega/2\Gamma$	$\omega/2\kappa$	κ/Γ
Re{ϵ} = 147.7, m = 2	3	2478	1989	46.9 (47.5)	42.4 (35.0)
$\lambda/r\approx 20$	5	2411	1946	298.0 (298.0)	6.5 (5.6)
$Q^{abs}\approx 10093$	7	2196	1804	769.7 (770.2)	2.3 (2.2)
	10	**2017**	**1681**	**1714 (1601)**	**0.98 (1.04)**
Re{ϵ} = 65.6, m = 3	3	7972	4455	144 (140)	30.9 (34.3)
$\lambda/r\approx 10$	5	9240	4824	2242 (2083)	2.2 (2.3)
$Q^{abs}\approx 10096$	7	9187	4810	7485 (7417)	0.64 (0.65)

[0169] Note that even though particular embodiments are presented and analyzed above as examples of systems that use resonant electromagnetic coupling for wireless energy transfer, those of self-resonant conducting coils, capacitively-loaded resonant conducting coils and resonant dielectric disks, any system that supports an electromagnetic mode with its electromagnetic energy extending much further than its size can be used for transferring energy. For example, there can be many abstract geometries with distributed capacitances and inductances that support the desired kind of resonances. In any one of these geometries, one can choose certain parameters to increase and/or optimize $\sqrt{Q_1Q_2}/Q_\kappa$ or, if the Q's are limited by external factors, to increase and/or optimize for Q_κ.

[0170] System Sensitivity to Extraneous Objects

[0171] In general, the overall performance of particular embodiment of the resonance-based wireless energy-transfer scheme depends strongly on the robustness of the resonant objects' resonances. Therefore, it is desirable to analyze the resonant objects' sensitivity to the near presence of random non-resonant extraneous objects. One appropriate analytical model is that of "perturbation theory" (PT), which suggests that in the presence of an extraneous object e the field amplitude $a_1(t)$ inside the resonant object **1** satisfies, to first order:

$$\frac{da_1}{dt}=-i(\omega_1-i\Gamma_1)a_1+i(\kappa_{11-e}+i\Gamma_{1-e})a_1 \tag{11}$$

where again ω_1 is the frequency and Γ_1 the intrinsic (absorption, radiation etc.) loss rate, while κ_{11-e} is the frequency shift induced onto 1 due to the presence of e and Γ_{1-e} is the extrinsic due to e (absorption inside e, scattering from e etc.) loss rate. The first-order PT model is valid only for small perturbations. Nevertheless, the parameters κ_{11-e}, Γ_{1-e} are well defined, even outside that regime, if a_1 is taken to be the amplitude of the exact perturbed mode. Note also that interference effects between the radiation field of the initial resonant-object mode and the field scattered off the extraneous object can for strong scattering (e.g. off metallic objects) result in total radiation-Γ_{1-e}'s that are smaller than the initial radiation-Γ_1 (namely Γ_{1-e} is negative).

[0172] The frequency shift is a problem that can be "fixed" by applying to one or more resonant objects a feedback mechanism that corrects its frequency. For example, referring to FIG. **8***a*, in some embodiments each resonant object is provided with an oscillator at fixed frequency and a monitor which determines the frequency of the object. Both the oscillator and the monitor are coupled to a frequency adjuster which can adjust the frequency of the resonant object by, for example, adjusting the geometric properties of the object (e.g. the height of a self-resonant coil, the capacitor plate spacing of a capacitively-loaded loop or coil, the dimensions of the inductor of an inductively-loaded rod, the shape of a dielectric disc, etc.) or changing the position of a non-resonant object in the vicinity of the resonant object. The frequency adjuster determines the difference between the fixed frequency and the object frequency and acts to bring the object frequency into alignment with the fixed frequency. This technique assures that all resonant objects operate at the same fixed frequency, even in the presence of extraneous objects.

[0173] As another example, referring to FIG. **8***b*, in some embodiments, during energy transfer from a source object to a device object, the device object provides energy to a load, and an efficiency monitor measures the efficiency of the transfer. A frequency adjuster coupled to the load and the efficiency monitor acts to adjust the frequency of the object to maximize the transfer efficiency.

[0174] In various embodiments, other frequency adjusting schemes may be used which rely on information exchange between the resonant objects. For example, the frequency of a source object can be monitored and transmitted to a device object, which is in turn synched to this frequency using frequency adjusters as described above. In other embodiments the frequency of a single clock may be transmitted to multiple devices, and each device then synched to that frequency.

[0175] Unlike the frequency shift, the extrinsic loss can be detrimental to the functionality of the energy-transfer scheme, because it is difficult to remedy, so the total loss rate $\Gamma_{1[e]}=\Gamma_1+\Gamma_{1-e}$ (and the corresponding figure-of-merit $\kappa_{[e]}/\sqrt{\Gamma_{1[e]}\Gamma_{2[e]}}$, where $\kappa_{[e]}$ the perturbed coupling rate) should be quantified.

[0176] Capacitively-Loaded Conducting Loops or Coils

[0177] In embodiments using primarily magnetic resonances, the influence of extraneous objects on the resonances is nearly absent. The reason is that, in the quasi-static regime of operation ($r \ll d$) that we are considering, the near field in the air region surrounding the resonator is predominantly magnetic (e.g. for coils with $h \ll 2r$ most of the electric field is localized within the self-capacitance of the coil or the externally loading capacitor), therefore extraneous non-conducting objects e that could interact with this field and act as a perturbation to the resonance are those having significant magnetic properties (magnetic permeability $\mathrm{Re}\{\mu\}>1$ or magnetic loss $\mathrm{Im}\{\mu\}>0$). Since almost all every-day non-conducting materials are non-magnetic but just dielectric, they respond to magnetic fields in the same way as free space, and thus will not disturb the resonance of the resonator. Extraneous conducting materials can however lead to some extrinsic losses due to the eddy currents induced on their surface.

[0178] As noted above, an extremely important implication of this fact relates to safety considerations for human beings. Humans are also non-magnetic and can sustain strong magnetic fields without undergoing any risk. A typical example, where magnetic fields $B \sim 1T$ are safely used on humans, is the Magnetic Resonance Imaging (MRI) technique for medical testing. In contrast, the magnetic near-field required in typical embodiments in order to provide a few Watts of power to devices is only $B \sim 10^{-4}T$, which is actually comparable to the magnitude of the Earth's magnetic field. Since, as explained above, a strong electric near-field is also not present and the radiation produced from this non-radiative scheme is minimal, it is reasonable to expect that our proposed energy-transfer method should be safe for living organisms.

[0179] One can, for example, estimate the degree to which the resonant system of a capacitively-loaded conducting-wire coil has mostly magnetic energy stored in the space surrounding it. If one ignores the fringing electric field from the capacitor, the electric and magnetic energy densities in the space surrounding the coil come just from the electric and magnetic field produced by the current in the wire; note that in the far field, these two energy densities must be equal, as is always the case for radiative fields. By using the results for the fields produced by a subwavelength ($r \ll \lambda$) current loop (magnetic dipole) with $h=0$, we can calculate the ratio of electric to magnetic energy densities, as a function of distance D_P from the center of the loop (in the limit $r \ll D_P$) and the angle θ with respect to the loop axis:

$$\frac{u_e(x)}{u_m(x)} = \frac{\varepsilon_o |E(x)|^2}{\mu_o |H(x)|^2} = \frac{\left(1+\frac{1}{x^2}\right)\sin^2\theta}{\left(\frac{1}{x^2}+\frac{1}{x^4}\right)4\cos^2\theta + \left(1-\frac{1}{x^2}+\frac{1}{x^4}\right)\sin^2\theta}; \quad (12)$$

$$x = 2\pi\frac{D_p}{\lambda}$$

$$\Rightarrow \frac{\oiint_{S_p} u_e(x)\,dS}{\oiint_{S_p} u_m(x)\,dS} = \frac{1+\frac{1}{x^2}}{1+\frac{1}{x^2}+\frac{3}{x^4}};$$

$$x = 2\pi\frac{D_p}{\lambda},$$

where the second line is the ratio of averages over all angles by integrating the electric and magnetic energy densities over the surface of a sphere of radius D_p. From Eq. (12) it is obvious that indeed for all angles in the near field ($x \ll 1$) the magnetic energy density is dominant, while in the far field ($x \gg 1$) they are equal as they should be. Also, the preferred positioning of the loop is such that objects which may interfere with its resonance lie close to its axis ($\theta=0$), where there is no electric field. For example, using the systems described in Table 4, we can estimate from Eq. (12) that for the loop of $r=30$ cm at a distance $D_p=10r=3$ m the ratio of average electric to average magnetic energy density would be ~12% and at $D_p=3r=90$ cm it would be ~1%, and for the loop of $r=10$ cm at a distance $D_p=10r=1$ m the ratio would be ~33% and at $D_p=3r=30$ cm it would be ~2.5%. At closer distances this ratio is even smaller and thus the energy is predominantly magnetic in the near field, while in the radiative far field, where they are necessarily of the same order (ratio→>1), both are very small, because the fields have significantly decayed, as capacitively-loaded coil systems are designed to radiate very little. Therefore, this is the criterion that qualifies this class of resonant system as a magnetic resonant system.

[0180] To provide an estimate of the effect of extraneous objects on the resonance of a capacitively-loaded loop including the capacitor fringing electric field, we use the perturbation theory formula, stated earlier, $\Gamma_1 = e^{abs} = \omega_1/4 \cdot \int d^3 r \mathrm{Im}\{\in_e(r)\}|E_1(r)|^2/U$ with the computational FEFD results for the field of an example like the one shown in the plot of FIG. **5** and with a rectangular object of dimensions 30 cm×30 cm×1.5 m and permittivity $\in=49+16i$ (consistent with human muscles) residing between the loops and almost standing on top of one capacitor (~3 cm away from it) and find $Q_{c\text{-}h}{}^{abs} \sim 10^5$ and for ~10 cm away $Q_{c\text{-}h}{}^{abs} \sim 5 \cdot 10^5$. Thus, for ordinary distances (~1 m) and placements (not immediately on top of the capacitor) or for most ordinary extraneous objects e of much smaller loss-tangent, we conclude that it is indeed fair to say that $Q_{c\text{-}e}{}^{abs} \to \infty$. The only perturbation that is expected to affect these resonances is a close proximity of large metallic structures.

[0181] Self-resonant coils are more sensitive than capacitively-loaded coils, since for the former the electric field extends over a much larger region in space (the entire coil) rather than for the latter (just inside the capacitor). On the other hand, self-resonant coils are simple to make and can withstand much larger voltages than most lumped capacitors.

[0182] In general, different embodiments of resonant systems have different degree of sensitivity to external perturbations, and the resonant system of choice depends on the particular application at hand, and how important matters of sensitivity or safety are for that application. For example, for a medical implantable device (such as a wirelessly powered artificial heart) the electric field extent must be minimized to the highest degree possible to protect the tissue surrounding the device. In such cases where sensitivity to external objects or safety is important, one should design the resonant systems so that the ratio of electric to magnetic energy density u_e/u_m is reduced or minimized at most of the desired (according to the application) points in the surrounding space.

[0183] Dielectric Disks

[0184] In embodiments using resonances that are not primarily magnetic, the influence of extraneous objects may be of concern. For example, for dielectric disks, small, low-index, low-material-loss or far-away stray objects will induce small scattering and absorption. In such cases of small per-

turbations these extrinsic loss mechanisms can be quantified using respectively the analytical first-order perturbation theory formulas All perturbations

$$\Gamma_{1\text{-}e}{}^{rad}=\omega_1\int d^3r Re\{\in_e(r)\}|E_1(r)|^2/U$$

and

$$\Gamma_{1\text{-}e}{}^{abs}=\omega_1/4\cdot\int d^3r Im\{\in_e(r)\}|E_1(r)|^2/U$$

where $U=1/2\int d^3r\in(r)|E_1(r)|^2$ is the total resonant electromagnetic energy of the unperturbed mode. As one can see, both of these losses depend on the square of the resonant electric field tails E_1 at the site of the extraneous object. In contrast, the coupling rate from object **1** to another resonant object **2** is, as stated earlier,

$$\kappa=\omega_1/2\cdot\int d^3r\in_2(r)E_2^*(r)E_1(r)/\int d^3r\in(r)|E_1(r)|^2$$

and depends linearly on the field tails E_1 of 1 inside 2. This difference in scaling gives us confidence that, for, for example, exponentially small field tails, coupling to other resonant objects should be much faster than all extrinsic loss rates ($\kappa\gg\Gamma_{1\text{-}e}$), at least for small perturbations, and thus the energy-transfer scheme is expected to be sturdy for this class of resonant dielectric disks. However, we also want to examine certain possible situations where extraneous objects cause perturbations too strong to analyze using the above first-order perturbation theory approach. For example, we place a dielectric disk c close to another off-resonance object of large $Re\{\in\}$, $Im\{\in\}$ and of same size but different shape (such as a human being h), as shown in FIG. **9***a*, and a roughened surface of large extent but of small $Re\{\in\}$, $Im\{\in\}$ (such as a wall w), as shown in FIG. **9***b*. For distances $D_{h/w}/r=10^{-3}$ between the disk-center and the "human"-center or "wall", the numerical FDFD simulation results presented in FIGS. **9***a* and **9***b* suggest that, the disk resonance seems to be fairly robust, since it is not detrimentally disturbed by the presence of extraneous objects, with the exception of the very close proximity of high-loss objects. To examine the influence of large perturbations on an entire energy-transfer system we consider two resonant disks in the close presence of both a "human" and a "wall". Comparing FIG. **7** to FIG. **9***c*, the numerical FDFD simulations show that the system performance deteriorates from $\kappa/\Gamma_c\sim$1-50 to $\kappa[hw]/\Gamma_{c[hw]}\sim$0.5-10 i.e. only by acceptably small amounts.

[0185] Inductively-loaded conducting rods may also be more sensitive than capacitively-loaded coils, since they rely on the electric field to achieve the coupling.

[0186] System Efficiency

[0187] In general, another important factor for any energy transfer scheme is the transfer efficiency. Consider again the combined system of a resonant source s and device d in the presence of a set of extraneous objects e. The efficiency of this resonance-based energy-transfer scheme may be determined, when energy is being drained from the device at rate Γ_{work} for use into operational work. The coupled-mode-theory equation for the device field-amplitude is

$$\frac{da_d}{dt}=-i(\omega-i\Gamma_{d[e]})a_d+i\kappa_{[e]}a_s-\Gamma_{work}a_d, \tag{13}$$

where $\Gamma_{d[e]}=\Gamma_{d[e]}{}^{rad}+\Gamma_{d[e]}{}^{abs}=\Gamma_{d[e]}{}^{rad}+(\Gamma_d{}^{abs}+\Gamma_{d\text{-}e}{}^{abs})$ is the net perturbed-device loss rate, and similarly we define $\Gamma_{s[e]}$ for the perturbed-source. Different temporal schemes can be used to extract power from the device (e.g. steady-state continuous-wave drainage, instantaneous drainage at periodic times and so on) and their efficiencies exhibit different dependence on the combined system parameters. For simplicity, we assume steady state, such that the field amplitude inside the source is maintained constant, namely $a_s(t)=A_se^{-iwt}$, so then the field amplitude inside the device is $a_d(t)=A_de^{-iwt}$ with $A_d/A_s=i\kappa_{[e]}/(\Gamma_{d[e]}+\Gamma_{work})$. The various time-averaged powers of interest are then: the useful extracted power is $P_{work}=2\Gamma_{work}|A_d|^2$, the radiated (including scattered) power is $P_{rad}=2\Gamma_{s[e]}{}^{rad}|A_s|^2+2\Gamma_{d[e]}{}^{rad}|A_d|^2$[1], the power absorbed at the source/device is $P_{s/d}=2\Gamma_{s/d}{}^{abs}|A_{s/d}|^2$, and at the extraneous objects $P_e=2\Gamma_{s\text{-}e}{}^{abs}|A_s|^2+2\Gamma_{d\text{-}e}{}^{abs}|A_d|^2$. From energy conservation, the total time-averaged power entering the system is $P_{total}=P_{work}+P_{rad}+P_s+P_d+P_e$. Note that the reactive powers, which are usually present in a system and circulate stored energy around it, cancel at resonance (which can be proven for example in electromagnetism from Poynting's Theorem) and do not influence the power-balance calculations. The working efficiency is then:

$$\eta_{work}\equiv\frac{P_{work}}{P_{total}}=\frac{1}{1+\frac{\Gamma_{d[e]}}{\Gamma_{work}}\cdot\left[1+\frac{1}{fom_{[e]}^2}\left(1+\frac{\Gamma_{work}}{\Gamma_{d[e]}}\right)^2\right]}, \tag{14}$$

where $fom_{[e]}=\kappa_{[e]}/\sqrt{\Gamma_{s[e]}\Gamma_{d[e]}}$, is the distance-dependent figure-of-merit of the perturbed resonant energy-exchange system. To derive Eq. (14), we have assumed that the rate Γ_{supply}, at which the power supply is feeding energy to the resonant source, is $\Gamma_{supply}=\Gamma_{s[e]}+\kappa_2/(\Gamma_{d[e]}\Gamma_{work})$, such that there are zero reflections of the fed power P_{total} back into the power supply.

EXAMPLE

Capacitively-Loaded Conducting Loops

[0188] Referring to FIG. **10**, to rederive and express this formula (14) in terms of the parameters which are more directly accessible from particular resonant objects, e.g. the capacitively-loaded conducting loops, one can consider the following circuit-model of the system, where the inductances L_s, L_d represent the source and device loops respectively, R_s, R_d their respective losses, and C_s, C_d are the required corresponding capacitances to achieve for both resonance at frequency ω. A voltage generator V_g is considered to be connected to the source and a work (load) resistance R_w to the device. The mutual inductance is denoted by M.

[0189] Then from the source circuit at resonance ($\omega L_s=1/\omega C_s$):

$$V_g=I_sR_s-j\omega MI_d\Rightarrow\frac{1}{2}V_g^*I_s=\frac{1}{2}|I_s|^2R_s+\frac{1}{2}j\omega MI_d^*I_s,$$

and from the device circuit at resonance ($\omega L_d=1/\omega C_d$):

$$0=I_d(R_d+R_w)-j\omega MI_s\Rightarrow j\omega MI_s=I_d(R_d+R_w)$$

S_0 by substituting the second to the first:

$$\frac{1}{2}V_g^*I_s=\frac{1}{2}|I_s|^2R_s+\frac{1}{2}|I_d|^2(R_d+R_w).$$

Now we take the real part (time-averaged powers) to find the efficiency:

$$\begin{aligned} P_g &= \mathrm{Re}\left\{\frac{1}{2}V_g^* I_s\right\} \\ &= P_s + P_d + P_w \Rightarrow \eta_{work} \\ &\equiv \frac{P_w}{P_{tot}} \\ &= \frac{R_w}{\left|\frac{I_s}{I_d}\right|^2 \cdot R_s + R_d + R_w}. \end{aligned}$$

Namely,

[0190]

$$\eta_{work} = \frac{R_w}{\frac{(R_d + R_w)^2}{(\omega M)^2} \cdot R_s + R_d + R_w},$$

which with $\Gamma_{work}=R_w/2L_d$, $\Gamma_d=R_d/2L_d$, $\Gamma_s=R_S/2L_s$, and $\kappa=\omega M/2\sqrt{L_sL_d}$, becomes the general Eq. (14). [End of Example]

[0191] From Eq. (14) one can find that the efficiency is optimized in terms of the chosen work-drainage rate, when this is chosen to be $\Gamma_{work}/\Gamma_{[e]}=\Gamma_{supply}/\Gamma_{s[e]}=\sqrt{1+/\mathrm{fom}_{[e]}^2}>1$. Then, η_{work} is a function of the $\mathrm{fom}_{[e]}$ parameter only as shown in FIG. **11** with a solid black line. One can see that the efficiency of the system is $\eta>17\%$ for $\mathrm{fom}_{[e]}>1$, large enough for practical applications. Thus, the efficiency can be further increased towards 100% by optimizing $\mathrm{fom}_{[e]}$ as described above. The ratio of conversion into radiation loss depends also on the other system parameters, and is plotted in FIG. **5** for the conducting loops with values for their parameters within the ranges determined earlier.

[0192] For example, consider the capacitively-loaded coil embodiments described in Table 4, with coupling distance D/r=7, a "human" extraneous object at distance D_h from the source, and that $P_{work}=10$ W must be delivered to the load. Then, we have (based on FIG. **11**) $Q_{s[h]}^{rad}=Q_{d[h]}^{rad}\sim10^4$, $Q_s^{abs}=Q_d^{abs}\sim10^3$, $Q_\kappa\sim500$, and $Q_{d\text{-}h}^{abs}\rightarrow\infty$, $Q_{s\text{-}h}^{abs}\sim10^5$ at $D_h\sim3$ cm and $Q_{s\text{-}h}^{abs}\sim5\cdot10^5$ at $D_h\sim10$ cm. Therefore $\mathrm{fom}_{[h]}\sim2$, so we find $\eta\approx38\%$, $P_{rad}\approx1.5$ W, $P_S\approx11$ W, $P_d\approx4$ W, and most importantly $\eta_h\approx0.4\%$, $P_h=0.1$ W at $D_h\sim3$ cm and $\eta_h\approx0.1\%$, $P_h=0.02$ W at $D_h\sim10$ cm.

[0193] Overall System Performance

[0194] In many cases, the dimensions of the resonant objects will be set by the particular application at hand. For example, when this application is powering a laptop or a cell-phone, the device resonant object cannot have dimensions larger that those of the laptop or cell-phone respectively. In particular, for a system of two loops of specified dimensions, in terms of loop radii $r_{s,d}$ and wire radii $a_{s,d}$, the independent parameters left to adjust for the system optimization are: the number of turns $N_{s,d}$, the frequency f, the work-extraction rate (load resistance) Γ_{work} and the power-supply feeding rate Γ_{supply}.

[0195] In general, in various embodiments, the primary dependent variable that one wants to increase or optimize is the overall efficiency η. However, other important variables need to be taken into consideration upon system design. For example, in embodiments featuring capacitively-loaded coils, the design may be constrained by, for example, the currents flowing inside the wires $I_{s,d}$ and the voltages across the capacitors $V_{s,d}$. These limitations can be important because for ~Watt power applications the values for these parameters can be too large for the wires or the capacitors respectively to handle. Furthermore, the total loaded $Q_{tot}=\omega L_d/(R_d+R_w)$ of the device is a quantity that should be preferably small, because to match the source and device resonant frequencies to within their Q's, when those are very large, can be challenging experimentally and more sensitive to slight variations. Lastly, the radiated powers $P_{rad,s,d}$ should be minimized for safety concerns, even though, in general, for a magnetic, non-radiative scheme they are already typically small.

[0196] In the following, we examine then the effects of each one of the independent variables on the dependent ones. We define a new variable wp to express the work-drainage rate for some particular value of $\mathrm{fom}_{[e]}$ through $\Gamma_{work}/\Gamma_{d[e]}=\sqrt{1+\mathrm{wp}\cdot\mathrm{fom}_{[e]}^2}$. Then, in some embodiments, values which impact the choice of this rate are: $\Gamma_{work}/\Gamma_{d[e]}=1\Leftrightarrow\mathrm{wp}=0$ to minimize the required energy stored in the source (and therefore I_s and V_{work}), $\Gamma_{work}/\Gamma_{d[e]}=\sqrt{1+\mathrm{fom}_{[e]}^2}>1\Leftrightarrow\mathrm{wp}=1$ to increase the efficiency, as seen earlier, or $\Gamma_{work}/\Gamma_{d[e]}\Leftrightarrow1\gg\mathrm{wp}\ll1$ to decrease the required energy stored in the device (and therefore I_d and V_d) and to decrease or minimize $Q_{tot}=\omega L_d/(R_d+R_w)=\omega/[2(\Gamma_d+\Gamma_{work})]$. Similar is the impact of the choice of the power supply feeding rate Γ_{supply}, with the roles of the source and the device reversed.

[0197] Increasing N_s and N_d increases $\kappa/\sqrt{\Gamma_s\Gamma_d}$ and thus efficiency significantly, as seen before, and also decreases the currents I_s and I_d, because the inductance of the loops increases, and thus the energy

$$U_{s,d} = \frac{1}{2}L_{s,d}|I_{s,d}|^2$$

required for given output power P_{work} can be achieved with smaller currents. However, increasing N_d increases Q_{tot}, $P_{rad,d}$ and the voltage across the device capacitance V_d, which unfortunately ends up being, in typical embodiments one of the greatest limiting factors of the system. To explain this, note that it is the electric field that really induces breakdown of the capacitor material (e.g. 3 kV/mm for air) and not the voltage, and that for the desired (close to the optimal) operational frequency, the increased inductance L_d implies reduced required capacitance C_d, which could be achieved in principle, for a capacitively-loaded device coil by increasing the spacing of the device capacitor plates d_d and for a self-resonant coil by increasing through h_d the spacing of adjacent turns, resulting in an electric field ($\approx V_d/d_d$ for the former case) that actually decreases with N_d; however, one cannot in reality increase d_d or h_d too much, because then the undesired capacitance fringing electric fields would become very large and/or the size of the coil might become too large; and, in any case, for certain applications extremely high voltages are not desired. A similar increasing behavior is observed for the source $P_{rad,s}$ and V_s upon increasing N_s. As a conclusion, the number of turns N_s and N_d have to be chosen the largest possible (for efficiency) that allow for reasonable voltages, fringing electric fields and physical sizes.

[0198] With respect to frequency, again, there is an optimal one for efficiency, and Q_{tot} is approximately maximum, close to that optimal frequency. For lower frequencies the currents get worse (larger) but the voltages and radiated powers get better (smaller). Usually, one should pick either the optimal frequency or somewhat lower.

[0199] One way to decide on an operating regime for the system is based on a graphical method. In FIG. **12**, for two loops of r_s=25 cm, r_d=15 cm, h_s=h_d=0, a_s=a_d=3 mm and distance D=2 m between them, we plot all the above dependent variables (currents, voltages and radiated powers normalized to 1 Watt of output power) in terms of frequency and N_d, given some choice for wp and N_s. The Figure depicts all of the dependencies explained above. We can also make a contour plot of the dependent variables as functions of both frequency and wp but for both N_s and N_d fixed. The results are shown in FIG. **13** for the same loop dimensions and distance. For example, a reasonable choice of parameters for the system of two loops with the dimensions given above are: N_s=2, N_d=6, f=10 MHz and wp=10, which gives the following performance characteristics: η_{work}=20.6%, Q_{tot}=1264, I_s=7.2 A, I_d=1.4 A, V_s=2.55 kV, V_d=2.30 kV, $P_{rad,s}$=15 W, $P_{rad,d}$ 0.006 W. Note that the results in FIGS. **12** and **13**, and the just above calculated performance characteristics are made using the analytical formulas provided above, so they are expected to be less accurate for large values of N_s, N_d, still they give a good estimate of the scalings and the orders of magnitude.

[0200] Finally, one could additionally optimize for the source dimensions, since usually only the device dimensions are limited, as discussed earlier. Namely, one can add r_s and a_s in the set of independent variables and optimize with respect to these too for all the dependent variables of the problem (we saw how to do this only for efficiency earlier). Such an optimization would lead to improved results.

[0201] Experimental Results

[0202] An experimental realization of an embodiment of the above described scheme for wireless energy transfer consists of two self-resonant coils of the type described above, one of which (the source coil) is coupled inductively to an oscillating circuit, and the second (the device coil) is coupled inductively to a resistive load, as shown schematically in FIG. **14**. Referring to FIG. **14**, A is a single copper loop of radius 25 cm that is part of the driving circuit, which outputs a sine wave with frequency 9.9 MHz. s and d are respectively the source and device coils referred to in the text. B is a loop of wire attached to the load ("light-bulb"). The various κ's represent direct couplings between the objects. The angle between coil d and the loop A is adjusted so that their direct coupling is zero, while coils s and d are aligned coaxially. The direct coupling between B and A and between B and s is negligible.

[0203] The parameters for the two identical helical coils built for the experimental validation of the power transfer scheme were h=20 cm, a=3 mm, r=30 cm, N=5.25. Both coils are made of copper. Due to imperfections in the construction, the spacing between loops of the helix is not uniform, and we have encapsulated the uncertainty about their uniformity by attributing a 10% (2 cm) uncertainty to h. The expected resonant frequency given these dimensions is f_0=10.56±0.3 MHz, which is about 5% off from the measured resonance at around 9.90 MHz.

[0204] The theoretical Q for the loops is estimated to be ~2500 (assuming perfect copper of resistivity $\rho=1/\sigma=1.7\times 10^{-8}$ Ωm) but the measured value is 950±50. We believe the discrepancy is mostly due to the effect of the layer of poorly conducting copper oxide on the surface of the copper wire, to which the current is confined by the short skin depth (~20 μm) at this frequency. We have therefore used the experimentally observed Q (and $\Gamma_1=\Gamma_2=\Gamma=\omega/(2Q)$ derived from it) in all subsequent computations.

[0205] The coupling coefficient κ can be found experimentally by placing the two self-resonant coils (fine-tuned, by slightly adjusting h, to the same resonant frequency when isolated) a distance D apart and measuring the splitting in the frequencies of the two resonant modes in the transmission spectrum. According to coupled-mode theory, the splitting in the transmission spectrum should be $\Delta\omega=2\sqrt{\kappa^2-\Gamma^2}$. The comparison between experimental and theoretical results as a function of distance when the two the coils are aligned coaxially is shown in FIG. **15**.

[0206] FIG. **16** shows a comparison of experimental and theoretical values for the parameter κ/Γ as a function of the separation between the two coils. The theory values are obtained by using the theoretically obtained κ and the experimentally measured Γ. The shaded area represents the spread in the theoretical κ/Γ due to the ~5% uncertainty in Q.

[0207] As noted above, the maximum theoretical efficiency depends only on the parameter $\kappa/\sqrt{\Gamma_1\Gamma_2}=\kappa/\Gamma$, plotted as a function of distance in FIG. **17**. The coupling to loss ratio κ/Γ is greater than 1 even for D=2.4 m (eight times the radius of the coils), thus the system is in the strongly-coupled regime throughout the entire range of distances probed.

[0208] The power supply circuit was a standard Colpitts oscillator coupled inductively to the source coil by means of a single loop of copper wire 25 cm in radius (see FIG. **14**). The load consisted of a previously calibrated light-bulb, and was attached to its own loop of insulated wire, which was in turn placed in proximity of the device coil and inductively coupled to it. Thus, by varying the distance between the light-bulb and the device coil, the parameter Γ_{work}/Γ was adjusted so that it matched its optimal value, given theoretically by $\sqrt{1+\kappa^2/(\Gamma_1\Gamma_2)}$. Because of its inductive nature, the loop connected to the light-bulb added a small reactive component to Γ_{work} which was compensated for by slightly retuning the coil. The work extracted was determined by adjusting the power going into the Colpitts oscillator until the light-bulb at the load was at its full nominal brightness.

[0209] In order to isolate the efficiency of the transfer taking place specifically between the source coil and the load, we measured the current at the mid-point of each of the self-resonant coils with a current-probe (which was not found to lower the Q of the coils noticeably.) This gave a measurement of the current parameters I_1 and I_2 defined above. The power dissipated in each coil was then computed from $P_{1,2}=\Gamma L|I_{1,2}|^2$, and the efficiency was directly obtained from $\eta=P_{work}/(P_1+P_2+P_{work})$. To ensure that the experimental setup was well described by a two-object coupled-mode theory model, we positioned the device coil such that its direct coupling to the copper loop attached to the Colpitts oscillator was zero. The experimental results are shown in FIG. **17**, along with the theoretical prediction for maximum efficiency, given by Eq. (14).

[0210] Using this embodiment, we were able to transfer significant amounts of power using this setup, fully lighting up a 60 W light-bulb from distances more than 2 m away, for example. As an additional test, we also measured the total power going into the driving circuit. The efficiency of the

wireless transfer itself was hard to estimate in this way, however, as the efficiency of the Colpitts oscillator itself is not precisely known, although it is expected to be far from 100%. Nevertheless, this gave an overly conservative lower bound on the efficiency. When transferring 60 W to the load over a distance of 2 m, for example, the power flowing into the driving circuit was 400 W. This yields an overall wall-to-load efficiency of ~15%, which is reasonable given the expected ~40% efficiency for the wireless power transfer at that distance and the low efficiency of the driving circuit.

[0211] From the theoretical treatment above, we see that in typical embodiments it is important that the coils be on resonance for the power transfer to be practical. We found experimentally that the power transmitted to the load dropped sharply as one of the coils was detuned from resonance. For a fractional detuning $\Delta f/f_0$ of a few times the inverse loaded Q, the induced current in the device coil was indistinguishable from noise.

[0212] The power transfer was not found to be visibly affected as humans and various everyday objects, such as metallic and wooden furniture, as well as electronic devices large and small, were placed between the two coils, even when they drastically obstructed the line of sight between source and device. External objects were found to have an effect only when they were closer than 10 cm from either one of the coils. While some materials (such as aluminum foil, styrofoam and humans) mostly just shifted the resonant frequency, which could in principle be easily corrected with a feedback circuit of the type described earlier, others (cardboard, wood, and PVC) lowered Q when placed closer than a few centimeters from the coil, thereby lowering the efficiency of the transfer.

[0213] We believe that this method of power transfer should be safe for humans. When transferring 60 W (more than enough to power a laptop computer) across 2 m, we estimated that the magnitude of the magnetic field generated is much weaker than the Earth's magnetic field for all distances except for less than about 1 cm away from the wires in the coil, an indication of the safety of the scheme even after long-term use. The power radiated for these parameters was ~5 W, which is roughly an order of magnitude higher than cell phones but could be drastically reduced, as discussed below.

[0214] Although the two coils are currently of identical dimensions, it is possible to make the device coil small enough to fit into portable devices without decreasing the efficiency. One could, for instance, maintain the product of the characteristic sizes of the source and device coils constant.

[0215] These experiments demonstrated experimentally a system for power transfer over medium range distances, and found that the experimental results match theory well in multiple independent and mutually consistent tests.

[0216] We believe that the efficiency of the scheme and the distances covered could be appreciably improved by silver-plating the coils, which should increase their Q, or by working with more elaborate geometries for the resonant objects. Nevertheless, the performance characteristics of the system presented here are already at levels where they could be useful in practical applications.

APPLICATIONS

[0217] In conclusion, we have described several embodiments of a resonance-based scheme for wireless non-radiative energy transfer. Although our consideration has been for a static geometry (namely κ and Γ_e were independent of time), all the results can be applied directly for the dynamic geometries of mobile objects, since the energy-transfer time κ^{-1} (~1 μs-1 ms for microwave applications) is much shorter than any timescale associated with motions of macroscopic objects. Analyses of very simple implementation geometries provide encouraging performance characteristics and further improvement is expected with serious design optimization. Thus the proposed mechanism is promising for many modern applications.

[0218] For example, in the macroscopic world, this scheme could potentially be used to deliver power to for example, robots and/or computers in a factory room, or electric buses on a highway. In some embodiments source-object could be an elongated "pipe" running above the highway, or along the ceiling.

[0219] Some embodiments of the wireless transfer scheme can provide energy to power or charge devices that are difficult or impossible to reach using wires or other techniques. For example some embodiments may provide power to implanted medical devices (e.g. artificial hearts, pacemakers, medicine delivery pumps, etc.) or buried underground sensors.

[0220] In the microscopic world, where much smaller wavelengths would be used and smaller powers are needed, one could use it to implement optical inter-connects for CMOS electronics, or to transfer energy to autonomous nano-objects (e.g. MEMS or nano-robots) without worrying much about the relative alignment between the sources and the devices. Furthermore, the range of applicability could be extended to acoustic systems, where the source and device are connected via a common condensed-matter object.

[0221] In some embodiments, the techniques described above can provide non-radiative wireless transfer of information using the localized near fields of resonant object. Such schemes provide increased security because no information is radiated into the far-field, and are well suited for mid-range communication of highly sensitive information.

[0222] A number of embodiments of the invention have been described. Nevertheless, it will be understood that various modifications may be made without departing from the spirit and scope of the invention.

What is claimed is:

1. A method, comprising:

forming a wireless power transfer system which uses at least two high-Q magnetically resonant elements, and

which have values which are set to acceptable levels of electric and magnetic field strength and radiated power.

2. A method as in claim **1**, wherein said acceptable levels comprise accepted standards for human safety.

3. A method as in claim **1**, wherein said acceptable levels comprise accepted standards for interference.

4. A method as in claim **1**, wherein said acceptable levels comprise accepted standards for both human safety and interference.

5. A method as in claim **1**, wherein said wireless power transfer is carried out at 13.56 MHz +/−7 kHz.

6. A method as in claim **1**, wherein said wireless transfer is carried out at 135 kHz.

7. A method as in claim **1**, wherein said wireless power transfer system creates fields that are higher than fields allowed by the standards, but are only higher than those standards in areas where a person cannot be located.

8. A method as in claim **1**, wherein said wireless power transfer system creates fields that are based both on biological effects and interference effects with other electronic devices.

9. A wireless power transfer system for transferring power to a high-Q receiver, comprising:

a high-Q transmitter which creates electric and magnetic field and radiated power levels that comply with acceptable levels in the region of operation.

10. A system as in claim **9**, wherein said acceptable levels for said transmitter are compliant with standards for human safety.

11. A system as in claim **9**, wherein said levels are compliant with accepted standards for interference.

12. A system as in claim **9**, wherein said levels are compliant with standards for both human safety and interference.

13. A system as in claim **9**, wherein said wireless power transfer is carried out at 13.56 MHz +/−7 kHz.

14. A system as in claim **9**, wherein said wireless power transfer is carried out at 135 kHz.

15. A system as in claim **9**, wherein said transmitter creates a level that is higher than the level of the standard, but is only in an area where a user cannot be located.

16. A system as in claim **9**, wherein said standards are standards both for biological effects, and also for interference effects.

17. A method as in claim **1**, wherein said standards are set by standard setting agencies.

18. A method as in claim **1**, wherein said standards are recommendations set by committees.

19. A method as in claim **1**, wherein said standards comprise both human safety and interference regulations and recommendations.

20. A system as in claim **9**, wherein said standards are set by standard setting agencies.

21. A system as in claim **9**, wherein said standards are recommendations set by committees.

22. A system as in claim **9**, wherein said standards comprise both human safety and interference regulations and recommendations.

* * * * *